Master's Thesis

TVVR 10/5018

Analysis of Climate Variability and Anthropogenic Impacts on the Water Balance of Lake Chad Drainage Basin

ELVIS ASONG ZILEFAC

Division of Water Resources Engineering

Department of Building and Environmental Technology

Lund University

Department of Water Resources Engineering

TVVR 10/5018

ISSN-1101-9824

Analysis of Climate Variability and Anthropogenic Impacts on the Water Balance of Lake Chad Drainage Basin

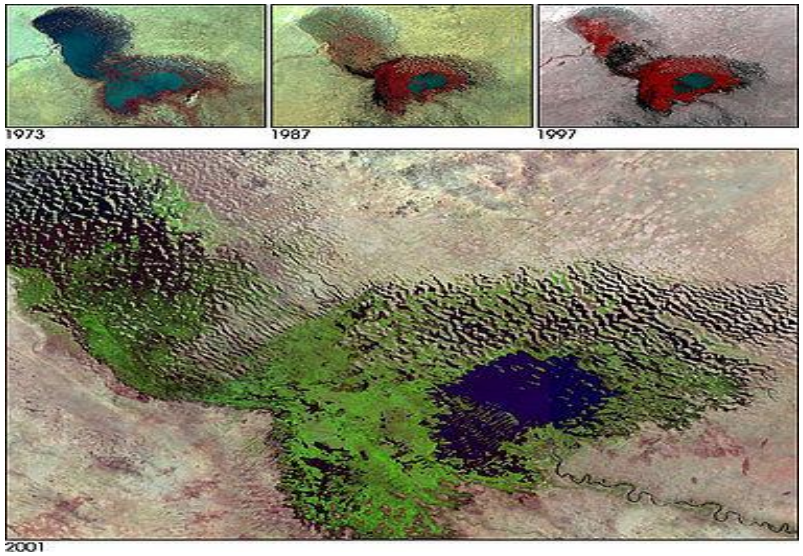

http://commons.wikimedia.org/wiki/File:ShrinkingLakeChad-1973-1997-EO.jpg

ELVIS ASONG ZILEFAC

Abstract

Sustainable utilization of scarce water resources requires a conceptualization and understanding of both local and regional climate variability. This work deals with an analysis of climate variability and human impacts on the water balance of the Lake Chad drainage basin of northern Africa. Mean annual precipitation and discharge time series from 112 rain gauges and monthly mean SST anomalies were used in this study to determine the influence of climate variability on precipitation and river discharge on Lake Chad. Multivariate statistical techniques were utilized to analyze the datasets.

Results showed that three EOFs explain spatial-temporal rainfall variability in the basin, accounting for 71% of the total variability in rainfall. The first EOF captures inter-annual rainfall fluctuations. The second EOF explains inter-decadal or long-term variability in precipitation. The third EOF explains rainfall variability to be driven by orographic configuration in the basin.Lake Chad drainage basin can be divided into three sub-regions of homogenous precipitation variability. Sub-region one depicts rainfall variability in the southernmost parts of the drainage basin and spread from west to east. Variability in rainfall at this sub-region is due mainly to the effect of topography on on-coming moisture bearing southwesterly monsoon winds. Sub-region two is mainly concentrated on the lee side of the Mandara and Adamawa mountain chains, the southwestern portions of the Djebel Mara in Sudan and north of Mongo hills in CAR. The inter-tropical convergence zone (ITCZ) brings summer rainfall in this sub-region. The third sub-region defines the northern Sahel - Saharan zone located between 13^{o}N-24^{o}N of the drainage basin. Rainfall variability is mainly a result of the formation of the African Easterly Jet (AEJ) over West Africa in summer due to strong meridional soil moisture gradients.

A component of precipitation variability in the basin owes its origin to SST anomalies in the tropical Atlantic Ocean. The first SVD heterogeneous mode has positive correlations in the far northeastern tropical Atlantic while the corresponding co-varying precipitation mode has positive correlations in the mid-southern portions of the Lake Chad catchment and negatively correlates with the rest of the basin. The second SVD mode has positive correlations in the lower northeastern tropical Atlantic while the corresponding precipitation field has positive correlations in the north-western portions of the Lake Chad catchment and negatively correlates with the rest of the basin.

By using precipitation as a predictor to discharge in the basin, a very high positive correlation is found with a strong linear relationship between the two fields during the study period. However, a monotonic trend analysis for discharge and precipitation between 1948 and 1988 showed most stations to have experienced significant negative trends and that precipitation decreased by 19% with the 1965-1988 period accounting 76% of the decrease while discharge decreased by 36% with the 1978-1988 period accounting 86.7% of the decrease. This implies climate variability though is responsible for fluctuating Lake Chad water balance, the amplitude of water resources degradation is exacerbated by other causes which could be of anthropogenic origin, accounting 17% (36% - 19%) of the discrepancy. It is recommended that there should be acquisition of high frequency climate data, recording daily evaporation and evapo-transpiration, an assessment of irrigation dams on major inflow rivers, types of irrigation practices, location of dams as well as their operation technologies.

Keywords: Lake Chad drainage basin; water balance; Climate Variability; precipitation; Discharge; SST anomalies; multivariate techniques; Regionalization; ITCZ; Trend analysis.

Title: Analysis of Climate Variability and Anthropogenic Impacts on the Water Balance of Lake Chad Drainage Basin

Author: Elvis Asong Zilefac

Supervisor: Prof. Cintia Bertacchi Uvo, Department of Water Resources Engineering

Problem: Lake Chad had once been the sixth world's largest lake and one of Africa's largest freshwater lakes before the early 1960s. Its surface area and water levels have fluctuated greatly after 1960. In the 1960s, the Lake surface area was about 25,000km^2 while in the wake of the 21st century, the Lake area dropped by 1/20th (23,650km^2) its size in the 1960s. Today, it boasts of 1,350km^2 only. Thus, the Lake shrunk about 90% its size between 1963 and 2001. It is about 1.5m deep today unlike 7m in 1963.

Aim: The main aim of this project is to identify the forces behind water resources degradation in the Lake Chad Basin through analysis of climate variability and anthropogenic impact on its water balance

Method: Cluster analysis (CA), Empirical Orthogonal Function analysis (EOF), Singular Value Decomposition (SVD), Canonical Correlation Analysis (CCA), Mann Kendall non-parametric trend test and Linear Regression

Conclusions: Climate variability though is responsible for fluctuating Lake Chad water balance, the amplitude of water resources degradation is exacerbated by other causes which could be of anthropogenic origin, accounting 17% (36% - 19%) of the discrepancy.

Keywords: Lake Chad drainage basin; water balance; Climate Variability; precipitation; Discharge; SST anomalies; multivariate techniques; Regionalization; ITCZ; Trend analysis.

Division of Water Resources Engineering
Department of Building and Environmental Technology

Faculty of Engineering, LTH
Lund University
P.O. Box 118, SE-221 00 Lund

Printed in Sweden, 2010

Preface

This thesis is based upon studies conducted from August 2009 to September 2010 at the department of Water resources Engineering, Lund university – Sweden. More than 6 months were centred on data collection and correction for missing values.

It all started in July 2008 when I applied for the Lot 10 Erasmus Mundus scholarship and was granted a place at Lund University. My able supervisor, Professor Cintia Bertacchi Uvo accepted this research proposal giving that climate plays a big role in water resources availability in Cameroon and Africa as a whole. The European Union provided me with a living allowance to study a master's degree during which I carried out this thesis.

At the beginning, the project success was bleak because data sets gathering were a major drawback. However, with encouragement, guidance and support from my supervisor, I became fascinated and determined to do this work.

The maps and figures in the project are drawn in ArcGIS and Matlab. Care must be taken to read the information conveyed in them. The resolution maybe low in some cases making them less comprehensible.

Acknowledgements

First and foremost, I am heartily thankful to my supervisor of this project, Professor Cintia Bertacchi Uvo, whose encouragement, guidance and support from the very beginning to the final level enabled me to develop an understanding of this project. She made available her support in a number of ways towards this project's success. This work would not have been possible without her at my disposal. I owe my greatest gratitude to her.

Besides, I would like to show my gratitude to the European Union for offering me a scholarship to undertake a master's degree in water resources at Lund University.

My sincere thanks also go to the authorities, professors and lecturers of the department of Water Resources Engineering for providing me with a good environment and facilities to complete this project.

Finally, an honourable mention goes to my family and friends. I deeply owe my father, Ndi Nkemasongafac Eric, my mother, Nkemasongafac Justine and all my brothers and sisters. Without the support of the above mentioned people, this project would not have been a success.

Elvis Asong Zilefac

Acronyms and Abbreviations

This work makes use of names of organisations and statistical methods. Here is a list of explanations to them:

AEJ: African Easterly jet

CA: Sub-region Analysis

CCA: Canonical Correlation Analysis

EOF: Empirical Orthogonal Function

GIWA: Global International Water Assessment

ITCZ: Inter-tropical Convergence Zone

IWRM: Integrated Water Resources Management

MK: Mann Kendall non-parametric Test

NSC: Normalized Squared Covariance

SCF: Squared Covariance fraction

SST: Sea Surface Temperature

SVD: Singular Value Decomposition

UNEP: United Nations Environmental Program

Table of Contents

1 Introduction

Sustainable utilization of scarce water resources requires a conceptualization and understanding of both local and regional climate variability. The Lake Chad is situated in a meridional zone of depression (GIWA, 2003) with marked micro-scale topographical configurations. This results in greater variability of rainfall owed to many factors accounting for its origin.

The causes of rainfall variability in the Sahel of Africa during the 1970s and 1980s have long been inferred. According to Nicholson (1979) and Lamb (1978), there have been several drought periods followed by wet episodes in African history. Is human activity to blame or is climate variability an issue which must be considered by stakeholders involved in the recovery of degrading Lake Chad water resources? Two parallel directions as to rainfall variability have been focussed upon: - the irreversible impact of human activities through land use changes and the atmospheric response to temperature changes in the global oceans as the leading cause of African climate variability (Chang *et al*., 2003).

The devastating droughts of the early 1970s and mid 1980s prompted researchers such as Lamb (1983), Lamb and Peppler (1992), Nicholson (1981) to look into possible mechanisms behind such temporal and spatial variability. Rainfall in semi-arid Africa has been noted for its inter-annual fluctuations, with greater impacts on the general hydrological cycle, water resources, food security and industries. This is typical of Africa south of the Sahara desert and north of the Sudan. Lake Chad is situated in this climate belt.

Le Barbe and Lebel (2001) carried out a study on rainfall variability in West Africa between 1950 and 1990 and noted a systematic decrease in the number of rainfall events which appeared well correlated to the decrease of mean inter-annual rainfall. Nicholson *et al.* (1992a) made an overview of Sahel rainfall fluctuations and found this region to have experienced decadal rainfall anomalies since the 1960s, depicting decreasing trends (Figure 1).

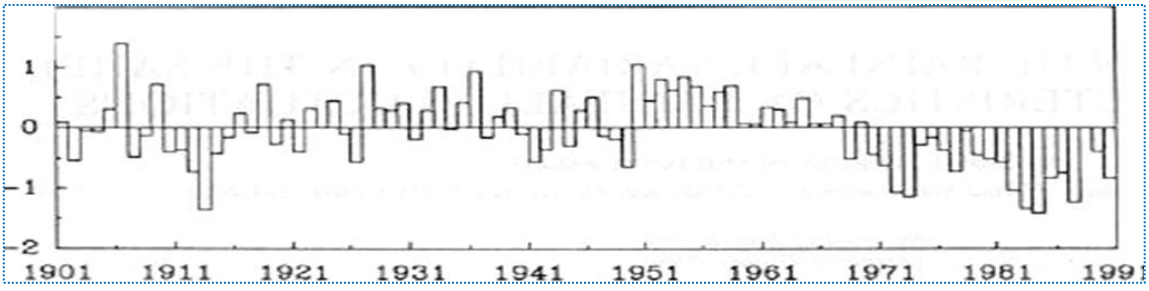

Figure 1:Long-term rainfall fluctuations in the Sahel of Africa (1901-1991). Rainfall remained generally below the mean from the early 1960s up to 1991 as depicted above.

Source: Nicholson (1992)

During the 1970 - 1990 period, rainfall remained below average across the semi-arid region and that in the northernmost section, 12^{o} N to about 20^{o} N, annual rainfall has exceeded the mean in only two years of the decade, 1988 and 1989. Due to negative trends of precipitation in the Sahel since the 1950s, Charney (1975) has made a speculation of a possible irreversible climate change which may have been a consequence of land surface degradation. It is worth noting that studies in this region of

Africa have shown rainfall to be increasing as of late 1990s. This is the case of Dai *et al*. (2004) who showed rainfall to have positive trends since late 1990s.

A deal of observational and General Circulation Models (GCM) experiments have shown that consistent patterns of sea surface temperature (SST) anomalies are associated with years of contrasting precipitation conditions in the Sahel (Lamb, 1978a, 1978b; Hastenrath, 1984; Lough, 1986; Fontaine and Bigot, 1993; Fontaine and Janicot, 1996; Fontaine *et al*., 1998). These relationships are valid for both annual and inter-decadal timescales (Hastenrath, 1990; Ward, 1998). Further studies through modeling provide further support for this paradigm (e.g. Folland *et al*., 1986, 1991; Rowell *et al*., 1992, 1995; Semazzi *et al*., 1996; Giannini *et al*., 2003).

Precipitation variability initiates variability in river flow. There exist coupled spatio - temporal inter-connections between precipitation, local topography, geology, soil types and groundwater recharge, and river flow. As precipitation is the lone meteorological input into the hydrologic cycle, it determines the dynamics in variability of the rest components. A critical analysis of precipitation patterns over a given drainage basin would serve a great deal of insight to ascertain the connection between groundwater recharge and long-term river discharge variability.

In order to understand the impact of climate variability on the water balance of the Lake Chad, cluster analysis (CA), Empirical Orthogonal Function analysis (EOF), Singular Value Decomposition (SVD), Canonical Correlation Analysis (CCA), Mann Kendall non-parametric trend test and Linear Regression were utilized. Several researchers have employed these techniques to solve similar meteorological and hydrological problems on temporal and spatial scales worldwide.

CA is applied to delineate homogenous rainfall variability regions. Uvo (2003) applied this technique to define areas of influence of the North Atlantic Oscillation on winter precipitation in northern Europe. Yurdanur *et al*. (2003) applied CA to divide Turkey into seven climatic zones and found that such zones had no clear–cut boundaries. Vincent *et al*. (2007) utilized CA in the regionalization of atmospheric variability in the western Sahel and eastern tropical North Atlantic during the boreal summer season and found eight homogenous climate regions.

Uvo (2003) applied EOF to seasonal precipitation totals to highlight principal patterns of variability in winter precipitation spanning the climatological characteristics of sub-regions in northern Europe. Nicholson *et al*. (1992a) utilized EOF in a re-evaluation of rainfall variability in the Sahel and identified primarily three spatial modes of rainfall variability in the region. The analysis also defined three broad homogenous sectors and rainfall variability within the sectors differed markedly. Chang *et al*. (2003) applied EOF to determine oceanic forcing of Sahel rainfall on inter-annual to inter-decadal time scales. They found out rainfall variability associated with the northern summer African monsoon to be dominated by two distinct modes that explain most of the rainfall variance. These patterns are well separated geographically, act on different time scales, and are linked to distinctively different patterns of SSTs.

Several researchers have also applied SVD and CCA in determining spatial and temporal patterns of precipitation variability due to oceanic forcing through SST anomalies. Uvo *et al*. (1998) applied SVD to show the relationships between Tropical Pacific and Atlantic SST and Northeast Brazil monthly precipitation. Zorita *et al.* (1992) applied CCA to show the relationship between Iberian precipitation, atmospheric circulation and SST in the North Atlantic area in winter. Preisendorfer *et al*. (1987) utilized CCA techniques to illustrate origins and levels of monthly and seasonal forecast skill for United Sates surface and air temperatures.

Most researchers have focused attention towards forecasting rainfall, runoff and stream flow using CCA (Uvo and Graham, 1998) and neural networks (Coulibaly *et al*., 2000) with little or no consideration for precipitation patterns driving such mechanisms. Such fundamental patterns of precipitation forcing through SSTs were studied by Uvo and Graham (1998) before runoff forecasting analysis. However, Westra *et al*. (2008) carried out a multivariate stream flow forecasting analysis using independent component analysis. Taha *et al*. (2001) performed a regional flood frequency estimation using CCA with little attention geared towards understanding at first sight the mechanisms behind stream flow variability for rivers in Ontario-Canada. Pilon and Cavadias (2002) applied the Mann Kendall non-parametric test to assess the significance of trends in annual maximum daily stream flow data of 20 pristine basins in Ontario, Canada.

However, all such studies have been on a broad-scale. None has been carried out in the Lake Chad drainage basin in particular aim at determining homogenous rainfall regions, modes of precipitation variability, showing dynamical inter-relationships between tropical SST anomalies and precipitation occurrence, relationships between precipitation and discharge variability as well as overall rainfall and discharge trends. This is relevant if one needs to understand the coupling between climate variability, recharge zones and hydrological inputs into the Lake Chad water body: - a pre-requisite for water balance quantification and management.

1.1 Background

Lake Chad with present surface area of 1,350km^2 is an endoheirc/terminal lake; implying that;

$$Qin + (p - e)A = \frac{dS}{dt}$$ where;

Qin = discharge/inflows; p = precipitation; e = evaporation; A = Lake cross-sectional area; dS = change in storage and dt = change in time scale. It occupies less than 1% of the topographic drainage basin (Coe and Foley, 2001). Its catchment is situated geographically between latitude 5-24^o N and longitude 7-25^o E (Figure 2) in the Sahel of North Africa.

Unlike most closed hydrological basins, the Lake Chad catchment is a freshwater system with river inflows and direct precipitation as inputs, and underground seepage and evaporation as natural outputs. With a topographic drainage basin area of 2,434,000km^2 and a hydrological drainage area of 966, 955km^2 stretching the boundaries of Chad, Cameroon, Niger, Nigeria, Libya, Algeria, Sudan and Central African Republic (CAR), it is situated at the edge of the Sahara desert.

The lake's bathymetry varies from North to South with major fluctuations in water levels and lake area since the 1960s (Figure 2).

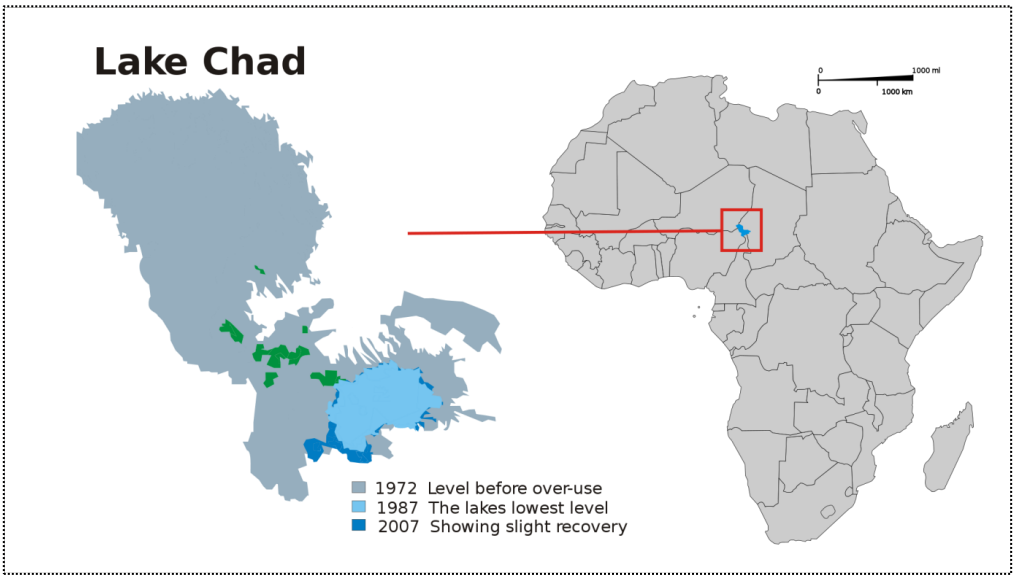

Figure 2: Illustrates the location of Lake Chad in Africa and the drainage basin. Three different surface areas are displayed. Note the explanation conveyed in the legend of the map. The green region represents wetland vegetation. (*http://commons.wikimedia.org/wiki/File:Lake_Chad_map_showing_receding_water_area_and_level_1972-2007.svg)*

Today, on the whole, it has an average depth of 1.5m (maximum depth of 8m), surface elevation of 280m and a water volume of about 72km^3.

1.1.1 Topography and Geology

Being a meridional zone of depression surrounded by hills (Figure 3), it is bounded to the North by the *Ahaggar* Mountains in Algeria, and the *Tibesti* highlands between Chad and Libya. In the South are the *Mongos* hills of CAR and the *Adamawa* and *Mandara* mountains of Cameroon, in the West is the Jos plateau , Nigeria and to the East by *Djebel Mara* in Sudan.

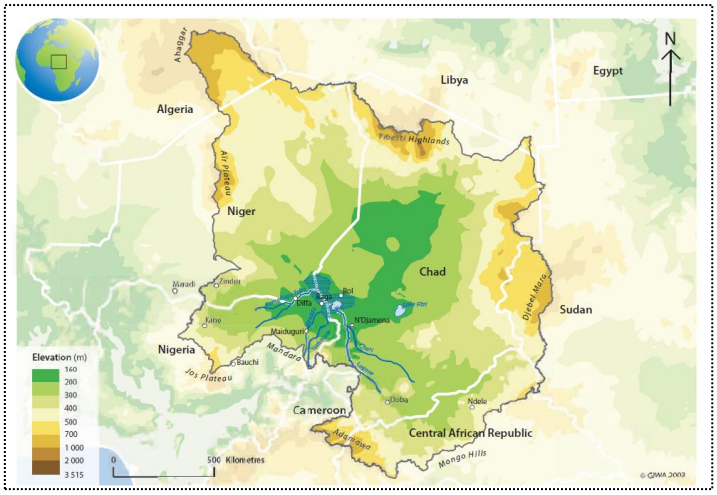

Figure 3: Illustrates the topography of the Lake Chad drainage basin. The southern portions of the basin are very hilly and act as geo-hydrological centers for inflows into the Lake Chad. The lake is situated in a depression within these hills. **Source:** GIWA, 2003.

The Lake Chad Basin was formed by extensional tectonic forces during the Cretaceous Period with the geological and geomorphologic development of the basin being conditioned by the slow and 'cool' rifting of the West and Central African rift System (GIWA, 2003). This formed a regional hydrological sink known as the Chad Artesian Basin that includes the Chad Syncline and the Chari-Logone Artesian Basin in the South-West of the basin. Significant reserves of groundwater in the basin are found in the alluvium of the Chari and Logone valleys. Much of the soil in the basin consists of clay particles which easily swell when wet, encouraging sheet wash rather than percolation into groundwater aquifers. However, the underlying aquifers comprise sandstones.

1.1.2 Climate and Hydrology

Climatologically, it has a monsoon climate, with majority of the precipitation occurring in the southern *1/3* of the basin, falling during the months of June, July and August. Arid conditions are widespread in the northern *2/3* (Coe and Foley, 2001). Precipitation across the Basin (located more in the Sahel) has experienced large variability in the last decades. The 1960s and 1970s were the driest decades due to a decrease in the number of large precipitation events (Nicholson, 1988, 2000). Mean annual precipitation fluctuates between 1500mm in the southern *1/3* of the basin to less than 100mm in the northern *2/3*. In the absence of orographic constraints, and considering atmospheric coupling, the reduction in precipitation is about 100mm for each 100km of distance northwards (Beauvilain, 1996).

The annual march of precipitation and the length of the rainy season south of the Sahara are solely dependent on the annual excursion of the Inter-tropical Convergence Zone (ITCZ) (Nicholson, 1980). The ITCZ is a zone of convergence of the trade winds. Surface easterlies prevail north of the thermal low, giving rise to harmattan dust laden winds that blow westward within the Sahara air layer into lake Chad basin, giving rise to the harsh dry months of November to April while moisture bearing southwesterly blow from the south bringing monsoon rainfall during northern Africa summer.

Main inflows to the lake include the *Chari*, *Logone* and rivers of the Komadougou –Yobe river system, all from the South (Figure 4). The Chari – Logone river system contribute about 90% of total inflows into the Lake Chad. The Chari and Logone Rivers flow into the Lake Chad at its southern extreme and flows northward and outwards encouraged by the Lake's gradient and prevailing winds.

These floodwaters take between one and two months to reach the southwest shore. The flow is at its minimum in May/June at the beginning of next year's rainy season (GIWA, 2003). The Chari – Logone river system is well drained. Various rivers flow as tributaries into this region. In particular are the Pende (a tributary of Logone) which becomes the Logone Oriental on reaching Chad. River Vina and Mbere feed the western branch of the Logone from Cameroon.

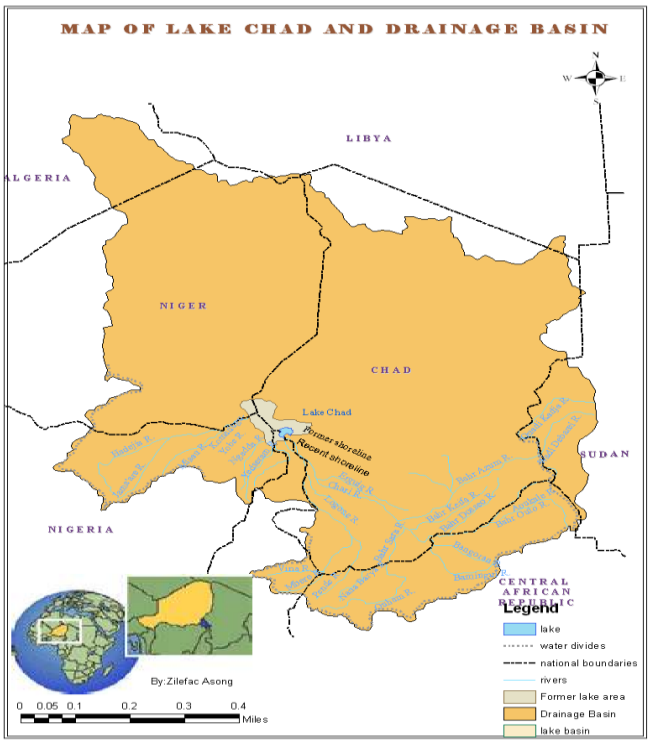

Figure 4: Location of study area in Northern Africa. The lake itself is situated in the Sahel zone of Africa. The drainage basin is shared between Cameroon, Chad, Nigeria, Algeria, Niger, Central African Republic, Libya, and Soudan. Rivers are only found in the southern part of the basin

The Yedseram and Ngadda rivers and their tributaries rise in the Mandara Hills (northern Cameroon) and they lose most of their waters while flowing northwards through a 7km wide flood plain. Further downstream of the Ngadda River (Nigeria) an 80km^2 swamp is formed from where the river does not maintain a definable watercourse to the Lake (GIWA, 2003). The system contains the Alau Dam (162 million m^3 reservoir), which is located southeast of Maiduguri in Nigeria.

The Komadugou-Yobe River system has a basin area of 148,000km^2 but contributes less than 2.5% of the total riverine inflow to Lake Chad. The Komadugou-Yobe River system is the border between Nigeria and Niger over the last 160km and is the only perennial river system flowing into the northern pool of Lake Chad. The Komadugou-Yobe is formed by various tributaries, in particular the Jama'are River which flows from the Jos Plateau (Nigeria), and the Hadejia River which flows from the area around Kano (Nigeria). The Hadejia River for the first 48km of its course maintains a gradient of approximately 1m/km. As it descends the gradient reduces abruptly with the channel diverging forming numerous oxbow lakes. The Jama'are begins with a relatively high gradient from the Jos Plateau before entering the Chad syncline northeast of Foggo (Nigeria). It is also supplied by the Misau, which comes from the north of Bauchi (Nigeria) and joins the Komadugou-Yobe River 120km from Lake Chad. Most of the headwaters carry a high sediment load of silt and fine sands that are deposited downstream, and there are resulting aggraded valleys of poorly defined channels with numerous small oxbow lakes (GIWA, 2003).

1.2 Problem Statement

One target of the United Nations millennium development goals is to "Halve, by 2015, the proportion of the population without sustainable access to safe drinking water and basic sanitation." Can inhabitants of the Lake Chad drainage basin meet this target when the only major water supply source is now sinking and at the verge of disappearing? In the IPCC's 2007 report on impacts, vulnerability and adaptation in Africa, there is no particular mention of the Lake Chad (Accessed on 7th September, 2010 at 19pm: http://www.ipcc.ch/pdf/assessment-report/ar4/wg2/ar4-wg2-chapter9.pdf). Lake Chad had once been the sixth world's largest lake and one of Africa's largest freshwater lakes before the early 1960s. Its surface area and water levels have fluctuated greatly after 1960. In the early 1960s, the Lake surface area was about 25,000km^2. Today, it boasts of 1,350km^2 only, meaning that the Lake area dropped by 1/20th (23,650km^2) its size since the 1960s. Thus, the Lake shrunk about 90% its size between 1963 and 2001 (Figure 5). It is about 1.5m deep today unlike 7m in 1963.

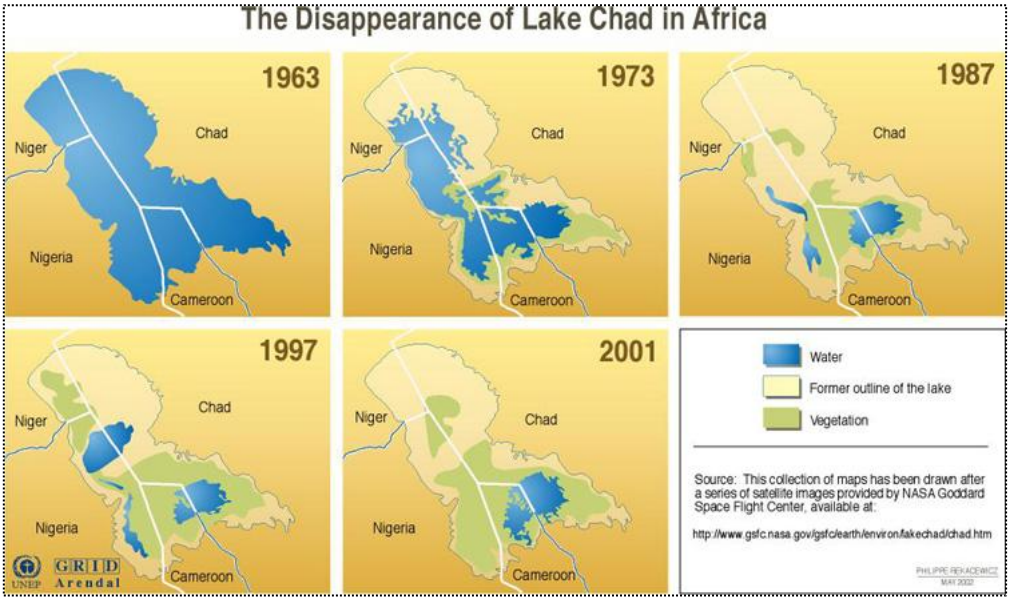

Figure 5: Drawings based on satellite images from NASA showing overtime variations in open water surface of the Lake Chad. It is evident that there is a high contrast between the area in 1963 and 2001. Today, water is available more on the eastern portions of the southern pool (source: http://www.grida.no/publications/vg/africa/page/3115.aspx)

The northern pool has not contained water for more than 25 years although there have been some flooding recorded during the wet years of 1994 and 1999 (GIWA, 2003). The implications of degrading water resources in the Lake are varied in many dimensions. More than 30 million people depend on it for water supply for domestic use, agriculture, livestock, fisheries, infant industries and navigation.

With the disappearance of the Lake at its present rate, there is a likelihood of an aggravating water stress already witnessed in the basin. Access to water supply for domestic use is poor and inefficient, utilizing traditional methods such as hand-dug wells to shallow depths. Thus, there is an urgent need for reversal of trends in water resources degradation in the Lake Chad drainage basin. In order to achieve this, the root causes of lake water disappearance must be sought so that water resources management in the basin would entail mitigating or adapting to such phenomena.

Several schools of thoughts have centered on climate change (Chang *et al*., 2003) and human impact on the ecology of the basin (Charney, 1975) as the causes of water resources degradation in the Sahel. Conclusions are not clear as to any single cause but an agglomeration of causes. Which of the above causes in the Lake Chad Basin is at the forefront is an option for scientific enquiry.

1.3 Aim, Objectives and Limitations

The main goal of this project is to identify the forces behind water resources degradation in the Lake Chad Basin through analysis of climate variability and anthropogenic impact on its water balance. In order to achieve this goal, specific objectives were set amongst which included the following;

- Identify changing patterns and modes of precipitation variability on an inter-annual basis across the basin between 1938 and 1993
- Characterization and delineation of homogenous precipitation sub-regions in the Lake Chad drainage basin of Northern Africa
- Examination of temporal inter-annual and spatial patterns of precipitation variability in the Lake Chad drainage basin and its link to SST anomalies in the Tropical Atlantic Ocean.
- Analysis of spatial-temporal relationships between precipitation and river discharge in the Lake Chad drainage basin
- Analysis of monotonic rainfall trends in the Lake Chad drainage basin and
- Analysis of river discharge trends in the Lake Chad drainage basin between 1948 and 1988.

In an attempt to achieve the aim and specific objectives of the study, some limitations were encountered. The study area is situated in one of the least developed regions in Africa. Up to date datasets were unavailable and the few available required higher costs for purchase. The datasets also had missing values which were filled using standard statistical methods. There was a time limitation for field work to be carried out aim at obtaining primary data. As such, all analyses were dependent on documented data and information in scholarly articles, journals, textbooks, consultations with the supervisor and the web.

2 Datasets Description

2.1 Precipitation

Monthly precipitation time series from rain gauges located between 5-24°N and 7-25°E were collected from the data library of the International Institute for Climate and Society (*http://iridl.ldeo.columbia.edu/anomaly.html*). Raw data consisted of monthly mean rainfall values spanning from 1904 -1993, spatially distributed as shown in Figure 6. In total, 113 meteorological stations had recorded rainfall data. However, due to the occurrence of missing data, the analysis was restricted to 1938-1993. The selected stations had at least 80% of observed data. One of the 113 stations did not fulfill this criterion and thus was dropped. The monthly means were summed to yearly averages of rainfall before analysis was made.

The dataset was corrected for missing values by replacing them with the long-term average for the specific month in a specific station. All stations are located at elevations between 111m and 1295m above mean sea level. It is evident from Figure 6 that the southern 2/3 of the basin has greater density of station network.

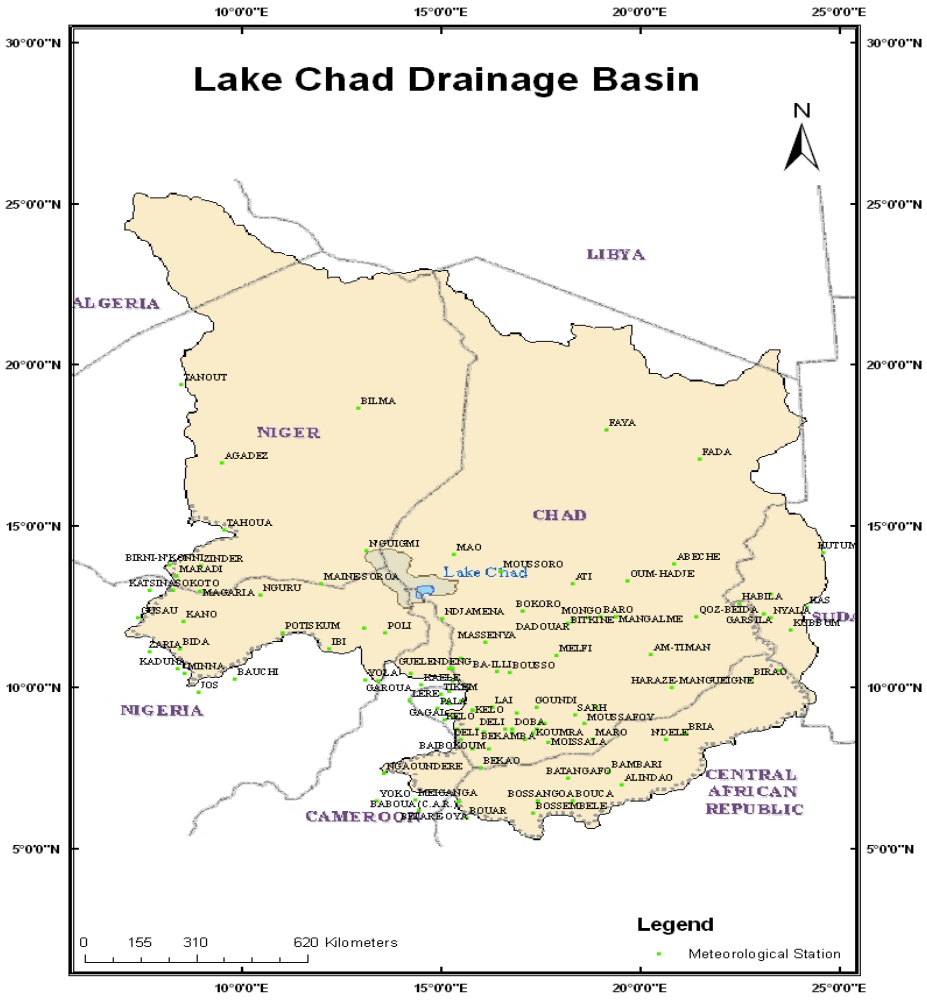

Figure 6: Location of meteorological stations utilized in the study. Station network density is greater over areas contributing inflow to the Lake Chad in the south. Green dots represent the stations while labels in black are World Meteorological Organization station names.

Prior to its use, annual totals time series were standardized (centered) by extracting the long-term mean for the given station and dividing by the standard deviation (Von Storch *et al*., 1995);

$$xi = (r - \tau)/\sigma$$

Where;

xi = rainfall expressed as standardized departure from the long-term mean

r = the rainfall total in the year

τ = the long-term mean of annual rainfall and

σ = standard deviation of rainfall totals from the mean.

The standardized rainfall series between 1938 and 1993 for the whole basin is shown on Figure 7;

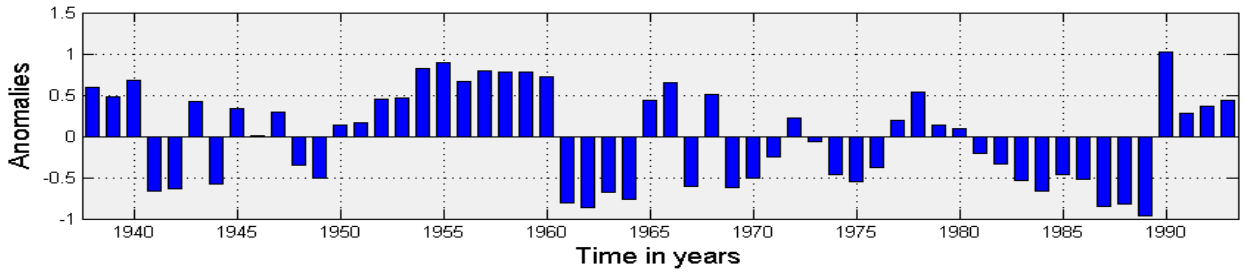

Figure 7: Evolution of the standardized rainfall anomalies over the Lake Chad drainage basin between 1938 and 1993. The 1950s were the wettest years in the basin but rainfall remained mostly below the mean from early 1960's to late 1980's.

2.2 Sea Surface Temperature

SST data consisted of statistically homogenous concatenation of Kaplan *et al*. (1998) OS SST dataset available at *http://iridl.ldeo.columbia.edu/SOURCES/.KAPLAN/.EXTENDED/.v2/* was utilized in this study. The data consists of time series of monthly mean SSTs from 1856-2010 with a spatial resolution of 5 degree latitude by 5 degree longitude. To investigate the roles of SST on precipitation variability, SST data was selected to have the same period as the precipitation data between 1938-1993, spanning the tropical Atlantic at latitude 30^{o}N to 20^{o}S and longitude 45^{o}W to 10^{o}E.
Since SST data was in monthly averages, it was summed to yearly averages to make it homogenous with yearly precipitation data. SST data was further standardized by extracting the mean and dividing by the standard deviation to show inter-annual anomalies/deviations from the central tendency (mean) (Figure 8).

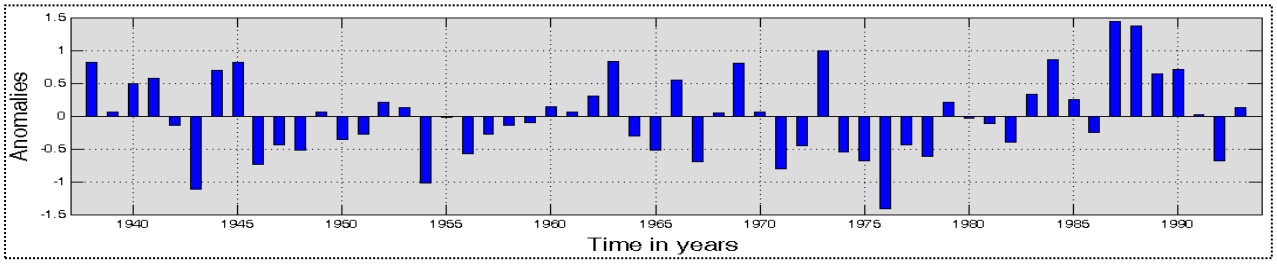

Figure 8: Evolution of the standardized SST anomalies over the Tropical Atlantic Ocean between 1938 and 1993. Note the similarity in anomalies between SST and precipitation between the 1960s and mid 1980s.

2.3 Stream flow/Discharge

Monthly averaged river discharge measurements from 15 ground - based gauge stations was collected from 1930 – 1991 and available at http://iridl.ldeo.columbia.edu/SOURCES/.UNH/.CSRC/.RivDIS/.dischrg/. The dataset was corrected for missing values by replacing them with the long-term average for the specific month in a specific station. To fulfill a 10% missing data criterion, the data set was down-scaled to the 1948 - 1988 period. Table 1 and Figure 9 show stations/rivers utilized in this study.

Table 1: Shows ground-based discharge stations, drainage areas of river basins and their elevations above mean sea level (msl), utilized in this work. Most of the stations are centered over the Chari-Logone Rivers which contribute most of the inflow to the Lake Chad

Station_no	Station_ID	area(km^2)	Country	Elevation(m)	Latitude	Longitude	River	Station_Name
1	4	1690	Cameroon	1048	7	13	Wina	Lahore
2	31	64000	Cameroon	174	9.3	13.38	Benoue	Garoua
3	38	600000	Chad	285	12.11	15.03	Chari	Ndjamona
4	42	193000	Chad	355	9.15	18.41	Chari	Sarh
5	1473	22800	Central African Republic	_	6.47	17.45	Ouham	Bossangoa
6	1474	96000	Central African Republic	_	9	19.15	Nahr Aouk	Golongoso
7	1476	44700	Central African Republic	_	7.3	18.28	Ouham	Batangafo
8	1478	73700	Chad	321	10.27	15.42	Logone	Bongor
9	1479	80000	Chad	_	11.03	20.28	Bahr Azoum	Am Timan
10	1480	450000	Chad	325	10.48	16.72	Chari	Bousso
11	1481	33970	Chad	391	8.53	16.07	Logone	Moundou
12	1482	14300	Chad	_	8.65	16.83	Pende	Doba
13	1483	56700	Chad	350	9.4	16.3	Logone	Lai
14	1484	67600	Chad	518	8.33	17.77	Bahr Sala	Moissala
15	1514	115000	Niger	298	13.28	12.6	Komadougou	Bagara Diffa

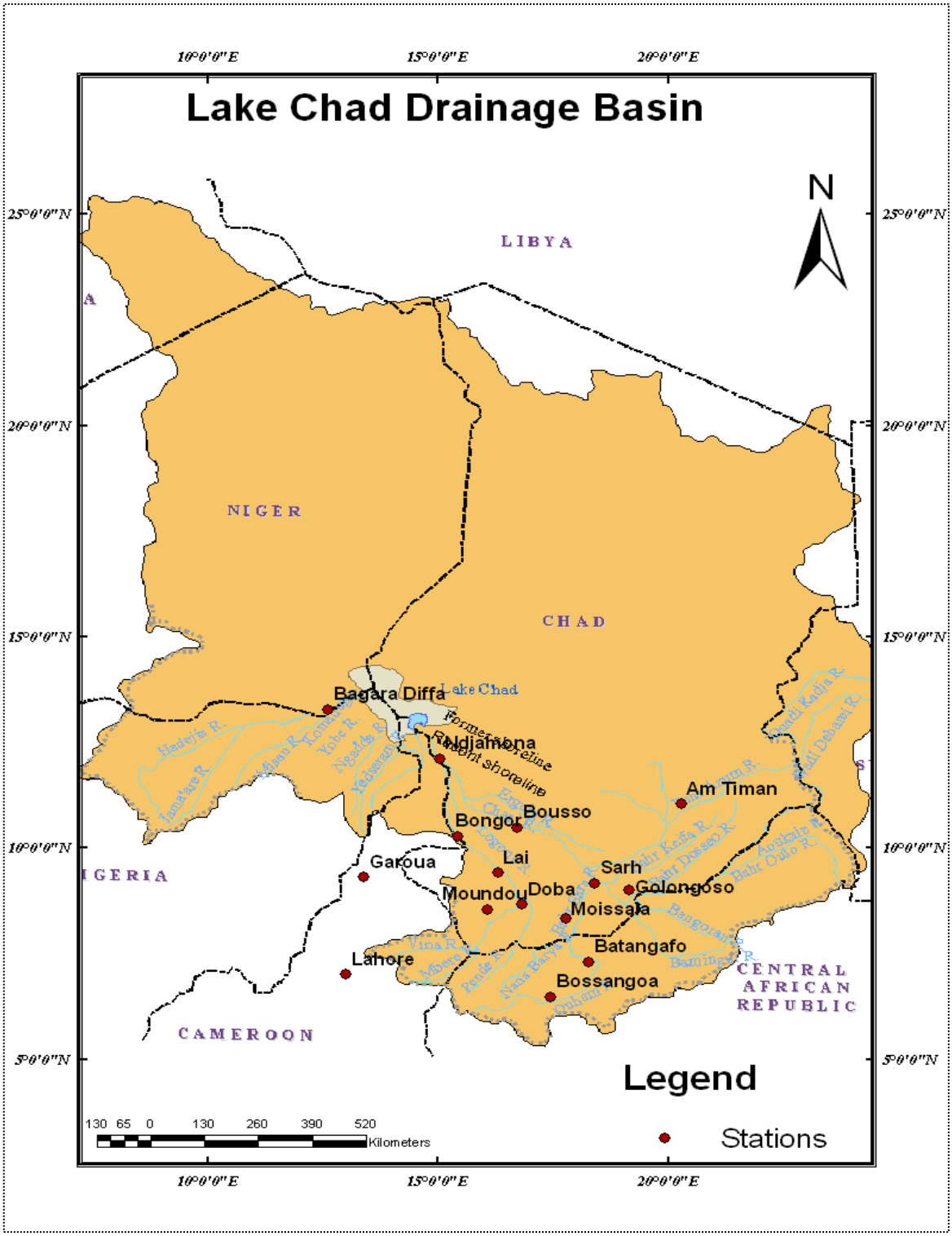

Figure 9: Illustrates discharge stations used in this study. All rivers are located in the southern 1/3 of the basin, mainly in the Southeast of the Lake Chad. To the West is the Komadugou river system with rivers originating from Western Mandara and Jos plateau. Red dots are stations; black labels represent station names while blue labels are rivers in the drainage basin

Figure 9 shows a map of the Lake Chad drainage basin, with its rivers and discharge gauge stations used in the study. Most rivers originate from the *Mongos* hills of CAR and the *Adamawa* and *Mandara* mountains of Cameroon in the South – Southeast; in the West, the Jos plateau in Nigeria and to the East, the *Djebel Mara* in Sudan.

Prior to its use, discharge data was standardized by extracting the mean and dividing by the standard deviation to show inter-annual anomalies/deviations from the long-term mean. The standardized and generalized river flow time series for all rivers between 1948 and 1988 is shown on Figure 10. The mean was extracted per river and divided by the standard deviation, and then an average of all rivers was taken to produce the generalized pattern on Figure 10.

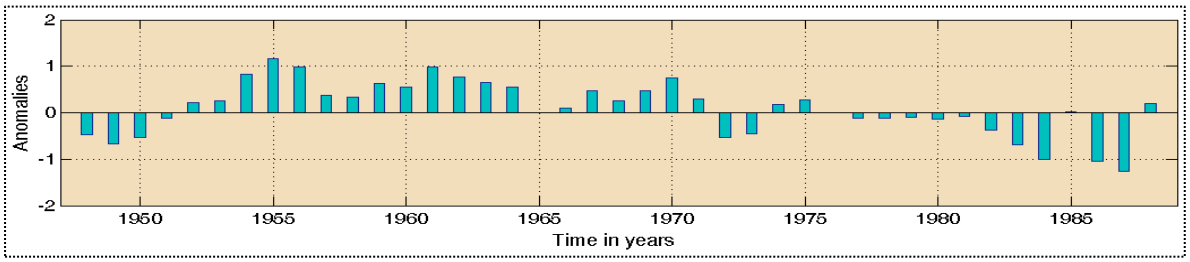

Figure 10: Illustrates the evolution of the standardized discharge anomalies of rivers in the Lake Chad drainage basin between 1948 and 1988. The 1950s and early 1960s were the high flow years in the basin but river discharge remained mostly below the mean from early 1970's to late 1980's.

Discharge has mostly been consistently below the mean since 1975 with the 1980s being the years with lowest discharges in the Lake Chad drainage basin.

3 Methods

Multivariate statistical techniques are utilized in this study to analyse secondary datasets described above. All analyses were performed in Matlab and ArcGIS.

3.1 Empirical Orthogonal Function Analysis (EOF)

In order to determine spatial variability of rainfall in the Lake Chad basin, EOF (also called principal component analysis) was applied to the annual precipitation time series. EOFs are defined as the eigenvectors of the covariance matrix derived from the time series of the data field (von Storch, 1995; Wilks, 1995). As a data reduction technique, EOF reduce a dataset containing a large number of variables to fewer variables, but that still represent a large fraction of the variability contained in the original dataset. Thus, it attempts to simplify a complex set of inter-relationships between variables by creating one or more new variables with respect to original ones that allow a convenient explanation of variability in the field. According to Richman, 1986; Preisendorfer, 1988; Graham, 1988, it aims at explaining the overall variance in a dataset by statistically isolating a number of components with respect to newly defined axes, with each corresponding to a variable.

Given the 112 rainfall stations, the pattern of variance within the data was complex to descend. This was then accomplished by applying EOF to the variance-covariance matrix generated from this data set; which identified 112 linear combinations of the original variables, known as EOF modes. The EOFs modes are orthogonal to each other, that is, are uncorrelated to each other. The proportion of the total variance associated with each of the EOF modes was determined mathematically as follows: let Z (precipitation) be the original dataset which is an M * N matrix. By computing a transformation of Z, say U which explains maximum variance (Variance (ZU) = maximum) between linear combinations of N_1, $N_3 \ldots N_n$ variables such that the transformed data, V = ZU and $\text{Variance}(V) = \frac{\sum(V*V)}{N-1} = \frac{V'V}{N-1} = \frac{(ZU)'ZU}{N-1} = \frac{U'Z'ZU}{N-1}$, but $\frac{Z'Z}{N-1}$ is the variance-covariance matrix, S, so that $\text{Variance}(V) = U'SU$. A maximization problem occurs where Variance (V) should be at maximum. By constraining U to unit length of 1 (U´U=1) and introducing a Lagrange multiplier, the maximization problem becomes; $\text{variance}(V) = f(U) = U'SU - \lambda(U'U - I) = \text{maximum}$ where; $\frac{\partial f(U)}{\partial U} = 0$ or $|S - \lambda I|\, U = 0$ (has the same structure as the characteristic equation that determines the eigen structure of a square matrix A; ($|A - \lambda I|E = 0$)). The variables E and λ contains the eigenvectors and eigenvalues respectively. This is interpreted to mean that the transformation that maximizes the variation of S is given by its eigenvectors, and the eigenmode with highest eigenvalue gives the transformation with the largest variance. Since U was constrained to unity, the total variance explained by each eigenmode is given by $\sum_{i=1}^{n} \lambda i$.

To relax the mathematical constrain of orthogonality and highlight the physical characteristics of each EOF mode, three EOF modes that together explained 71% of the total original variance were further subjected to orthogonal varimax rotation. Eigenvectors of the retained EOFs were then plotted on a map of the basin (Figures 11, 12, and 13) to show spatial variability of rainfall.

3.2 Cluster Analysis (CA)

Cluster analysis was utilized to define areas of similar rainfall variability. CA is used for grouping variables into subsets that are linearly related to each other (Uvo, 2003). Unlike other multivariate statistical methods, CA is not based on any *a priori* assumptions. Thus, greater attention must be tailored towards the choice of clustering method. In this study, hierarchical clustering methods were applied for exploratory data analysis (Wilks, 1995) since no theoretical assumptions was made *a priori*. Common metrics for CA are distance measures and correlation coefficients. Euclidean distance (the square root of the sum of squared distances over all variables) is most commonly used. Mahalanobis Distance: this uses the correlation coefficients between observations to cluster them (Wilks, 1995). Correlation coefficients have a drawback in that they lack sensitivity to the magnitude of the differences between the variables (Wilks, 1995).

All hierarchical methods follow four basic steps to find subsets that are both homogenous and well divided, that objects in every cluster are linearly related to each other:

- The specified distance measure between all meteorological stations is calculated
- The two closest stations are merged to form a new cluster depending on the type of clustering
- The distance between all stations is recalculated
- Steps two and three are repeated until all stations with similar characteristics are merged into one cluster.

There are five widely used hierarchical clustering methods: Ward's minimum distance, average distance, single linkage, complete linkage, and centroid method. According to Kalkstein et al., 1987, Ward's minimum variance method has been the most widely used clustering technique in climate research and was used in this study.

In this study, the dissimilarity measure applied is Euclidean distance. The data was standardized prior to distance calculation to eliminate the scale effect, since observations with different scales as rainfall may unequally play a role in the computed distance. Euclidean distance is defined as;

$$\mathrm{dij} = \frac{\mathrm{N}}{\mathrm{Mk}} = 1\mathrm{M}\ (\mathrm{xik} - \mathrm{xjk})2 \quad \text{(3-1)}$$

Where; dij is the Euclidean distance between xi and xj over M stations. N is the number of stations used in the study.

Before applying CA to define regions of similar variability, Empirical Orthogonal Function (EOF) analysis was employed to filter noise in the data. Only modes that explained 90% of variance in the dataset were retained for the CA. In CA, one of the main issues is to define the optimum number of clusters (at which step to stop). The method used here was by plotting the minimum distances between the combined clusters versus cluster numbers. This procedure gave guidance as to the optimum number of clusters. Sudden steps in distance reflect that the joining clusters are not similar.

This method was used to develop 'dendrograms' which are hierarchical tree-like diagrams showing relations among all variables (stations) in the dataset (Everitt, 1980). For more detailed mathematical techniques behind CA, see Wilks (1995).

3.3 Singular Value Decomposition (SVD)

In order to identify those precipitation patterns in the Lake Chad catchment that are forced by SST anomalies, singular value decomposition (SVD) after Bretherton *et al.* (1992) was applied to precipitation in the Lake Chad drainage basin and mean yearly SST anomalies in the Tropical Atlantic Ocean.

In this method, the left field or predictor (*Y*) is SST while the right field or predictand (*Z*) is precipitation. For more on predictor and predictand fields, refer to Wallace *et al*. (1992). SVD or Maximum Covariance Analysis is used first to identify dominant modes of co-variability between precipitation and SST. According to Bretherton *et al*., 1992, SVD decomposes the cross-covariance matrix of two data fields and identifies the pair of spatial patterns that explain the mean-squared temporal covariance between the two fields. It can explain the maximum possible fraction of the cumulative squared covariance with fewer leading modes than any other tool that is capable of isolating coupled modes of variability between the time series of two fields. SVD isolates linear combinations of variables within two fields that tend to be linearly related to one another (Wilks, 1995). It involves an eigenvector decomposition of the cross-covariance matrix between two input fields or variables.

Precipitation and SST time series were first standardized as shown in Figures 7 and 8 respectively. SVD was applied to the cross-covariance matrix, $Cyz = \frac{1}{nt-1} * Y'Z$, of the two datasets; $Y_{nt,ny}$ (left field) and $Z_{nt,nz}$ (right field) , where *nt* is the number of time steps and *ny* and *nz* the space/variable. Spatial patterns (eigenvectors), G and H, which are a linear combination from *Y* and *Z* data sets respectively and explained most of the total covariance between left (*Y*) and right (*Z*) field, were determined as $U = YG$ and $V = ZH$, where *U* and *V* are transformations from original time series of *Y* and *Z* data sets respectively.
G and *H* were chosen such that the covariance $(cov(U,V) = \frac{1}{nt-1} * U'V)$ between *U* and *V* are maximized. By solving a maximization problem resulting from the cross-covariance matrix between *Y* and *Z*, pairs of spatial patterns that explain most of the temporal covariance between the two fields; $G_{ny,\,k}$ and $H_{nz,\,k}$ (*k* = the mode of the singular vector) were identified. The new time series projected unto the new coordinate system was computed as $U_{nt,\,k} = Y_{nt,\,ny} * G_{ny,\,k}$ and $V_{nt,\,k} = Z_{nt,\,nz} * H_{nz,\,k.}$ Four (4) dominant SVD modes were retained for correlation and jointly explained 71% of the total covariance between *Y* and *Z*. When both fields are one and the same variable, SVD simply yields homogenous correlation maps which relate the expansion coefficient of the k_{th} mode to the time series of the same field/variable at each grid point or station.
Note that compared with EOF, SVD decomposes variability into modes, but in order of decreasing explained cross-covariance between variables in a field rather than of co-variance within a single variable field. In each mode, a pair of singular vectors describes spatial patterns of loadings for the two variables that relate to that mode. Likewise, time series (*U* and *V*) of expansion coefficients describe the weighting of the mode on the two variables in the corresponding temporal domain.

When both fields are of different variables, instead of homogenous correlation maps, a more diagnostic spatial relationship between variables in form of heterogeneous correlation maps for each mode is calculated and analyzed. The heterogeneous correlation map for each variable is a plot, over the corresponding spatial domain, of correlation coefficients between individual time series of one variable and the expansion coefficients of the other variable. Here, the heterogeneous correlation maps for the k_{th} SVD expansion mode indicate how accurate the pattern of SST anomaly relates to k_{th}

expansion coefficients of the precipitation field. The Normalized Squared Covariance (NSC) between Y and Z was also utilized in the analyses. It varies between 0 and 1. When it is 0, the two co-varying fields are unrelated and when it is 1, variations at each grid point/station in the left field are perfectly correlated with variations at all grid points/stations in the right field (Wallace et al., 1993).

3.4 Canonical Correlation Analysis (CCA)

For purposes of inter-comparison, CCA was applied to the same datasets of precipitation and SST. CCA is a linear method that has the main advantage of selecting pairs of spatial patterns that are optimally correlated, making a physical interpretation of connection between predictand and predictor possible. According to Preisendorfer *et al*. (1987), it is highly advisable to apply a data space reduction procedure prior to CCA. This was accomplished by projecting the data (*Y* and *Z*) onto EOFs and then retaining only a limited number of EOFs since CCA is linked to properties of the cross-covariance matrix, **C***zy*, and this procedure resolves the eigen-value problem while reducing noise in the dataset. For more mathematical procedures in CCA computations, refer to Preisendorfer *et al*. (1987) and Bretherton *et al.* (1992).

By applying EOF analysis, three dominant EOFs in the left, or predictor field (SST), were retained and jointly explained 78.58% of the original variance while two dominant EOFs were retained from the right or predictand field (precipitation) and explained 65% of the variance. The new time series projected on the new coordinates, $U_y = YE_y$ and $U_z = ZE_z$, where U_y and U_z are the projected time series of the left and right fields respectively; *Y* and *Z* are original time series of the left and right fields respectively and E_y and E_z are retained eigenmodes of Y and Z respectively. U_y and U_z were then used as input data to perform CCA. The time series (canonical vectors) of the canonical patterns (*U* and *V* transformed from *Y* and *Z* respectively) were computed. Canonical correlations (*g* and *h* for U and V respectively) were computed. These maps(*g* and *h*) show the correlations at specific locations between the new time series (canonical vectors) and the reconstructed time series from the EOF analysis. The new time series (U and V) and correlations (*g* and *h*) were plotted for visualisation. In all analyses, only correlations significant at 95% and 99% confidence level are shown.

3.5 Mann Kendall Test for Trends (MK)

Statistical procedures were applied to determine rainfall trends in the study area. Kendall (1975) describes a normal-approximation test that could be used for time series with greater than 10 values, provided there are limited tied values. The Mann Kendall non-parametric test was employed to detect the presence of monotonic trends in the data set. This test compares the relative magnitude of time series data rather than the data values themselves (Gilbert, 1987). Thus, the data need not conform to a particular distribution. The data values are evaluated as an ordered time series. Each value is compared to all subsequent data sets, with the net result of increments and decrements being the MK statistic, S, given by;

$$\sum_{k=1}^{n-1} \sum_{j=k+1}^{n} \mathbf{sign(xj - xk)} \quad \text{..... (3-2)}$$

Where;

Sign $(xj - xk) = 1$ if $xj - xk > 0$

$= 0$ if $xj - xk = 0$

$= -1$ if $xj - xk < 0$

If $S \neq 0$, a test of significance is conducted. The probability associated with S and the data size, n, was computed to statistically quantify the significance of the trend. A normalized test statistic, Z, was computed thus;

$$VAR\ (S) = \frac{n(n-1)(2n+5)}{18} \quad \text{..... (3-3)}$$

$$Z = S - \frac{1}{VAR(S)^{0.5}} \quad if\ S > 0$$

$$Z = 0 \quad if\ S = 0$$

$$Z = S + \frac{1}{VAR(S)^{0.5}} \quad if\ S < 0$$

The probability density function for a normal distribution with a mean of 0 and σ of 1 is denoted as $f(z) = 1/2\pi^{1/2}e^{-z2/2}$.

The trend is negative when Z is negative and the computed probability is greater than alpha and positive when Z is positive and the computed probability is greater than alpha. The statistical significance of the time series is tested at 95% confidence interval or 0.05 significance level (α). The null hypothesis: H_o → there is no trend is accepted if $-Z_{1-\alpha/2} \leq Z \leq Z_{1-\alpha/2}$ otherwise it is rejected in favour of the alternative hypothesis: H_1→ that there is a trend. At this significance level, a trend is said to be significant if the computed probability associated with S (not with Z) is less than α .The validity of Mann Kendall statistic (S) was supported through application of linear regression analysis. Both methods showed correspondence. A test for statistical significance of the regression is computed through application of the T-test statistic at 95% confidence bounds. To determine spatial variability of rainfall in the basin, coefficients of variation (the coefficient of variation (CV) is the ratio of the standard deviation to the mean (Rogerson, 2006)) were computed on a station basis as follows: as the data represented yearly mean values, these values were summed for each station, the mean computed, with the variance. The standard deviation was then the square root of its variance ($\sigma = \sqrt{\sigma^2}$) and $CV\ (\%) = \sqrt{\sigma^2}\ /\tau * 100$.

4 Results

4.1 Spatial Rainfall Patterns in the Lake Chad Drainage Basin using EOF

Results of EOF are shown in Figures 11, 12 and 13(red crosses show factor loadings >0.08, green crosses show loadings <0.08 and blue dashes show negative signals). From the analysis, three EOF eigenvectors are retained for interpretation (EOF 1= 45.9%; EOF 2 = 19.13%; and EOF 3 = 6.22%) and jointly explain 71% of the total variability in rainfall in the Lake Chad basin. The other modes each accounted for less than 3% of the variance and were dropped. Retained EOFs are chosen based on the eigenvalue, scree plot, proportion of variance accounted for, and the interpretability (Factor loadings on EOFs) of the results criteria.

The first EOF mode eigenvector (Figure 11) explains 45.9% of the total variability of precipitation in the drainage basin. This eigen-mode captures mostly inter-annual variability in rainfall. EOF 1 has like signs (positive crosses) over the entire analysis sector. However, the loadings represented in red on Figure 11B are about twice those in green. By inspecting Figure 11B, it is evident that larger values (red crosses) of eigenvector loadings are concentrated in the lee of the Adamawa, Mongo and the Djebel Mara mountain chains and parts of the northern flanks of Jos plateau in Nigeria. This demonstrates similarity in the inter-annual variability of rainfall in this region. This coincides well with sub-region two of CA (Figures 14 and 15B). This is the zone of greater intensity of convergence of the tropical easterly and the south-westerly within the ITCZ in summer at approximately 10^{o}N latitude.

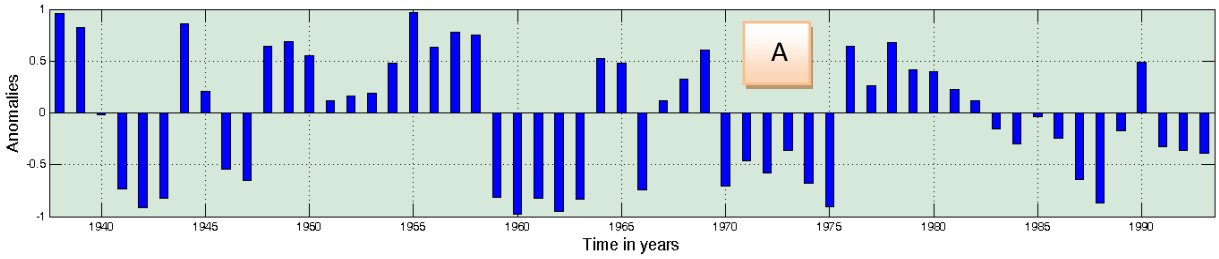

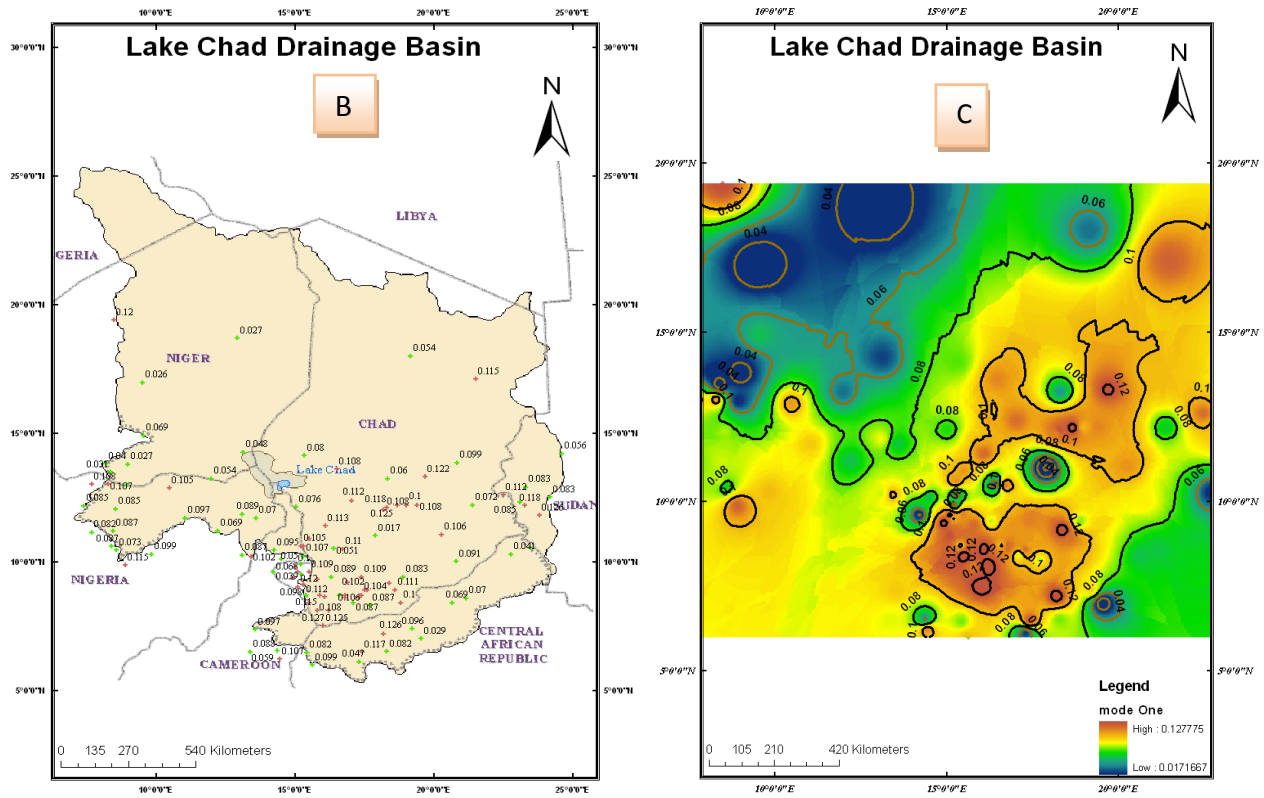

Figure 11: Illustrates eigen-vector loadings of the first spatial EOF (Explained variance = 45.9%). 11A show the corresponding EOF time series and 11B shows factor loadings for each station on EOF 1. while the raster image (11C) show results of interpolation of the loadings. Black isolines represent homogenous correlations significant at alpha level of 0.05 while the orange lines are significant at 0.01 alpha levels. Zero isolines are represented in white.

EOF 1 time series (Figure 11A) show a long decline of rainfall from the early 1960s throughout the late 1980s. The explanation conveyed in this eigen-mode is well depicted on Figure 11C.

The second EOF mode eigenvector explains 19.13% of the total rainfall variability in the Lake Chad basin. This mode explains inter-decadal or long-term variability as shown in Figure 12(A).

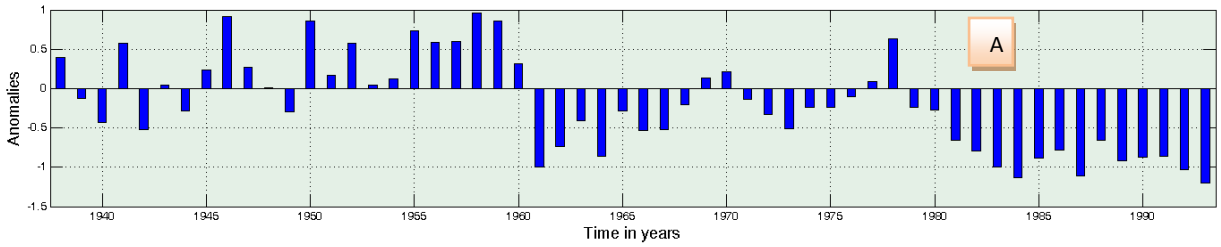

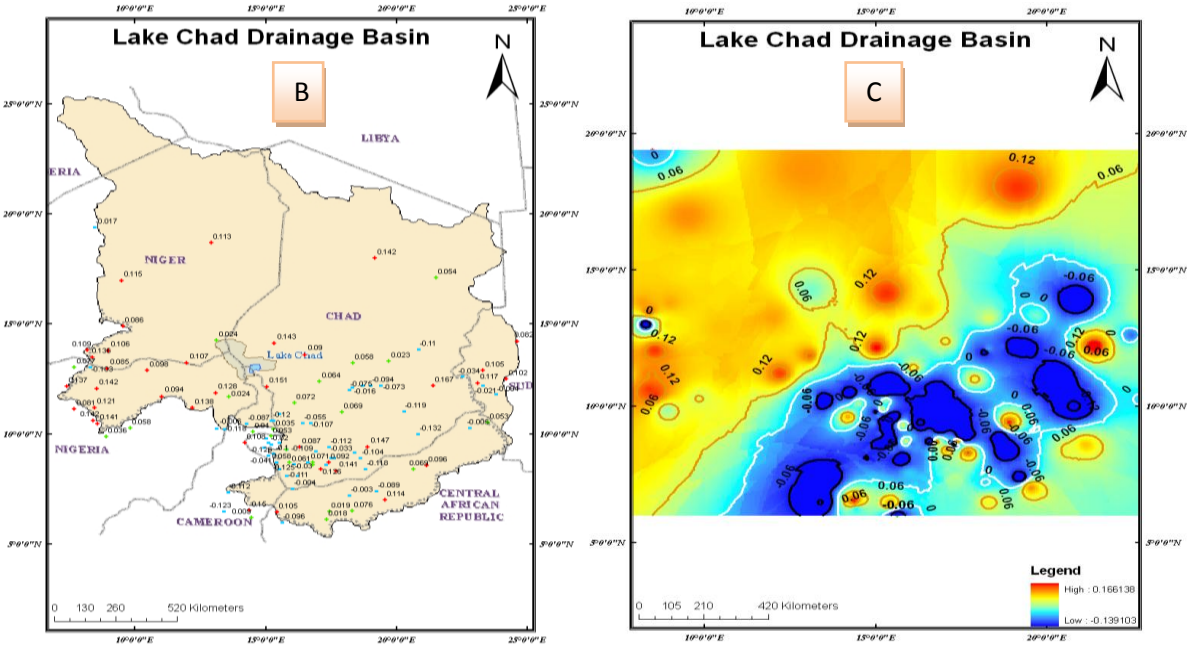

Figure 12: Illustrates eigenvector loadings of the second spatial EOF (Explained variance = 19.13%). 12A shows the corresponding EOF time series. The map (12B) shows areal distribution of such loadings while the raster image (12C) show results of interpolation of the loadings. Black isolines represent homogenous correlations significant at alpha level of 0.05 while the orange lines are significant at 0.01 alpha levels. Zero isolines are represented in white colour.

Figure 12B shows high positive signals (indicated in red crosses) to be located more between 13^{o}N-25^{o}N coinciding with the Sahel-Saharan region (sub-region three) identified in CA. Negative signals are loaded on the region identified in EOF 1 eigenvector mode. The corresponding EOF time series (12A) shows greater inter-decadal fluctuations in rainfall since the early 1950s and 1980s. This corresponds with the drought period in the Sahel. Variability in this region is mostly a result of the formation of the African Easterly Jet (AEJ) over West Africa in summer (July-October) as a result of strong meridional soil moisture gradients.

The third EOF eigenvector mode explains 6.22% of the variance. Figure 13 shows eigenvector loadings on this EOF.

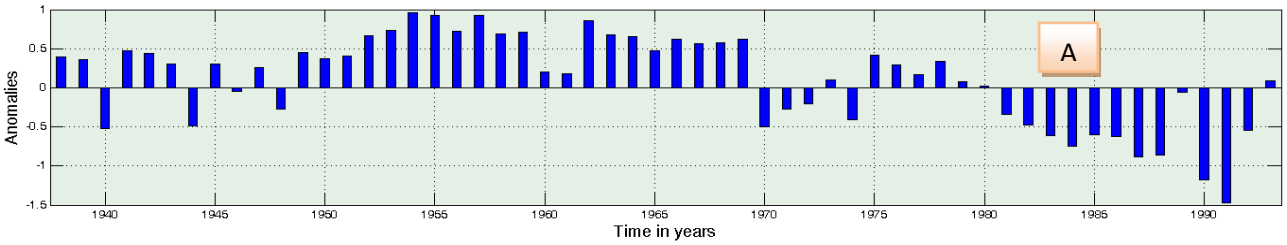

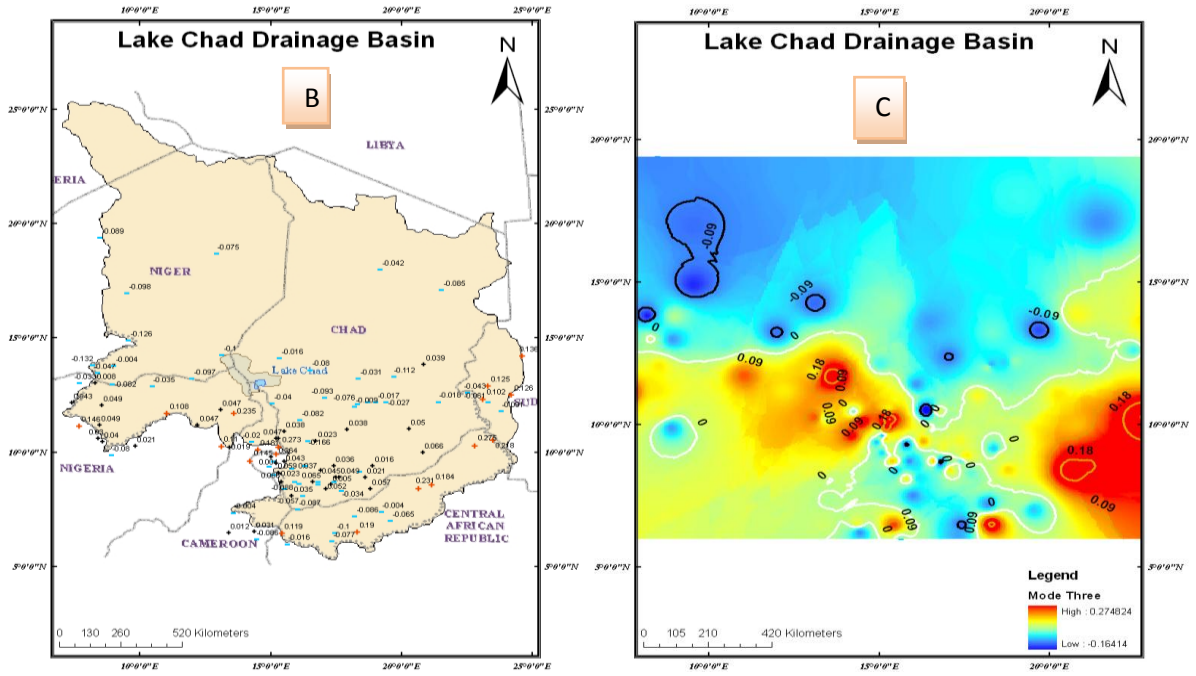

Figure 13: Illustrates eigenvector loadings of the third spatial EOF eigenvector (Explained variance = 6.22%). 13A shows the corresponding EOF time series. The map (13B) shows areal distribution of such loadings while the raster image (13C) show results of interpolation of the loadings. Black isolines represent homogenous correlations significant at alpha level of 0.05 while the orange lines are significant at 0.01 alpha levels. Zero isolines are represented in white colour.

As illustrated on Figure 13B, eigenvector loadings greater than 0.08 are represented by red crosses and the pattern is similar to topographic configuration shown on Figure 3. Larger eigenvector values are concentrated over the Adamawa and Mandara in Cameroon, Mongo Hills in CAR, Djebel Mara Mountains in Soudan and Jos and Air plateau in Nigeria and Niger respectively. Variability explained by the first EOF is negatively loaded (blue sign on Figure 13B) on EOF 2. Thus, EOF 1 explains variability not explained by EOF 2 and this is strongly evident on the raster image (Figure 13C). The long decline of rainfall since the late 1960s is strongly evident (Figure 13A). Eigen-vector 3 is consistently positive from 1938 to 1962 and consistently negative since then. This coincides strongly with sub-region one of CA.

To relax the orthogonality assumption and spread out the explained variance across the EOFs, varimax rotation (not shown here) was performed with EOFs 1, 2 and 3 having explained variances of 35.74%, 29.29% and 6.21% respectively. Rotation did not produce further significant results unlike un-rotated EOFs. It is worth noting that the results obtained from EOF are alike those obtained by using CA because prior to application of CA, the data is filtered for unwanted noise using EOF and only patterns in data that account for most of rainfall variability are used in the CA.

4.2 Discretization of Lake Chad Basin into homogenous Rainfall Regions

The results from CA are shown on Figures 14 and 15. Based on spatial rainfall variability, the Lake Chad basin is divided into three sub-regions as shown on Figure 14. Selected stations in each sub-region to explain variability of rainfall are shown in Table 2.

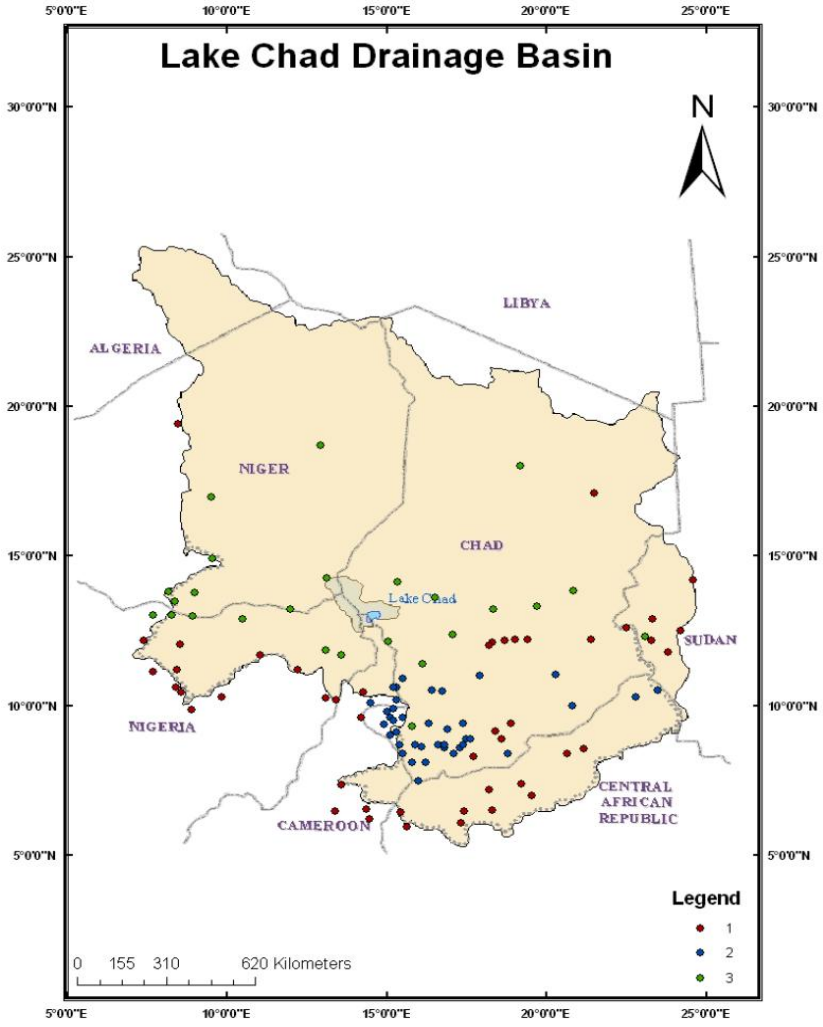

Figure 14: Illustrates three sub-regions defining homogenous rainfall variability regions in the basin. Red dots represent sub-region one, blue dots for sub-region two and green dots for sub-region three. The sub-regions have no well defined boundaries. Stations in each sub-region are not located in any single region of the basin except sub-region two due to varied topographic and physiographic configurations.

Table 2: shows selected stations from the three different sub-regions used for illustration of rainfall variability in the basin

	Sub-region one		
Station Name	Longitude	Latitude	Elevation
Ngaoundere	13.57	7.35	1114
Minna	8.55	10.45	262
Fada	21.5	17.1	-
Baboua	15.43	6.45	-

	Sub-region two		
Station Name	Longitude	Latitude	Elevation
Panzangue	15.8	8.1	-
Goundi	17.4	9.4	368
Kairoual	15.2	9.5	402
Radom	23.48	10.53	-

	Sub-region three		
Station Name	Longitude	Latitude	Elevation
Bilma	12.92	18.68	355
Faya	19.17	18	235
Ndjamena	15.03	12.13	295
Agadez	9.49	16.97	501

Worth noting is the grouping of the sub-regions, which occur in chunks, sparingly over the basin. The foregoing classifications of the Lake Chad drainage basin into three homogenous regions of rainfall variability stem from macro, meso to micro-scale atmospheric disturbances, land surface degradation as well as its natural location within the tropical latitudes.

Sub-region one (red dots) depicts rainfall variability in the southernmost parts of the drainage basin and spread from west to east. This is the zone of origin (geo-hydrological heads) of all tributaries to rivers feeding the Lake Chad (Figures 3 and 4). These stations are concentrated over the mountain chains of *Adamawa* and *Mandara* in Cameroon, *Jos* plateau in Nigeria, *Air* plateau in Niger, *Mongo* hills of CAR, *Djebel Mara* of Sudan and the *Tibesti* highlands of northern Chad.

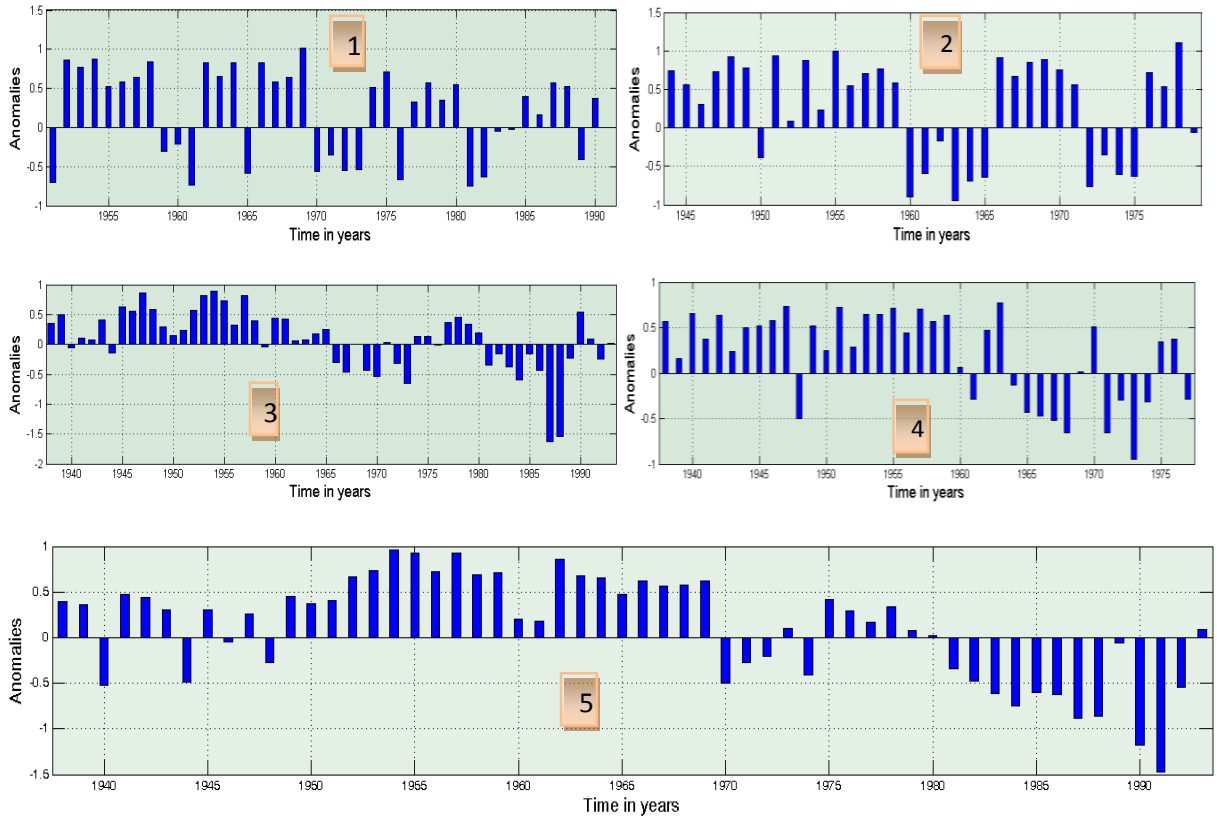

Figure 15A: Illustrates rainfall variability in sub-region one between 1938 and 1993. Most stations in this sub-region are located southernmost of the drainage basin where rainfall has been mostly above the mean for most of the years until the late 1960s when it dropped below the mean in Ngaoundere (1), Minna (2), Fada (3), and Baboua (4) and for the entire sub-region

one(5) since 1970s. Rainfall variability here is mainly due to topographic influence on southwesterly low monsoon winds from the Atlantic Ocean.

Figure 15A shows the evolution of the standardized rainfall anomaly between 1938 and 1993 over stations in this sub-region. Figure 15A1, A2, A3, A4 and A5 shows variability of rainfall in Ngaoundere, Minna, Fada, and Baboua and for the entire sub-region one. Rainfall in this region is of orographic origin as depicted from the mountain chains shown in Figure 3. During the northern African summer which starts earlier in the southern part of the drainage basin (April-October), southwesterly monsoon winds blowing from the tropical Atlantic Ocean drive moisture into the Lake Chad basin. Upon approaching these orographic features, these winds are displaced upward as they cool adiabatically, resulting in condensation on the windward portions of the mountain chains depicted in sub-region one and Figure 3. However, the moisture laden winds upon descending the Mandara and the Adamawa mountain chains in Cameroon, the Jos plateau in Nigeria, and the Mongo hills in CAR loss most of their moisture giving a rainfall regime eminent of sub-region two. The strength of these winds reduces from the southwest-southeast-northern direction.

Sub-region two (blue dots) is mainly concentrated on the lee of the Mandara and Adamawa mountain chains, the southwestern portions of the Djebel Mara in Sudan and north of Mongo hills in CAR.

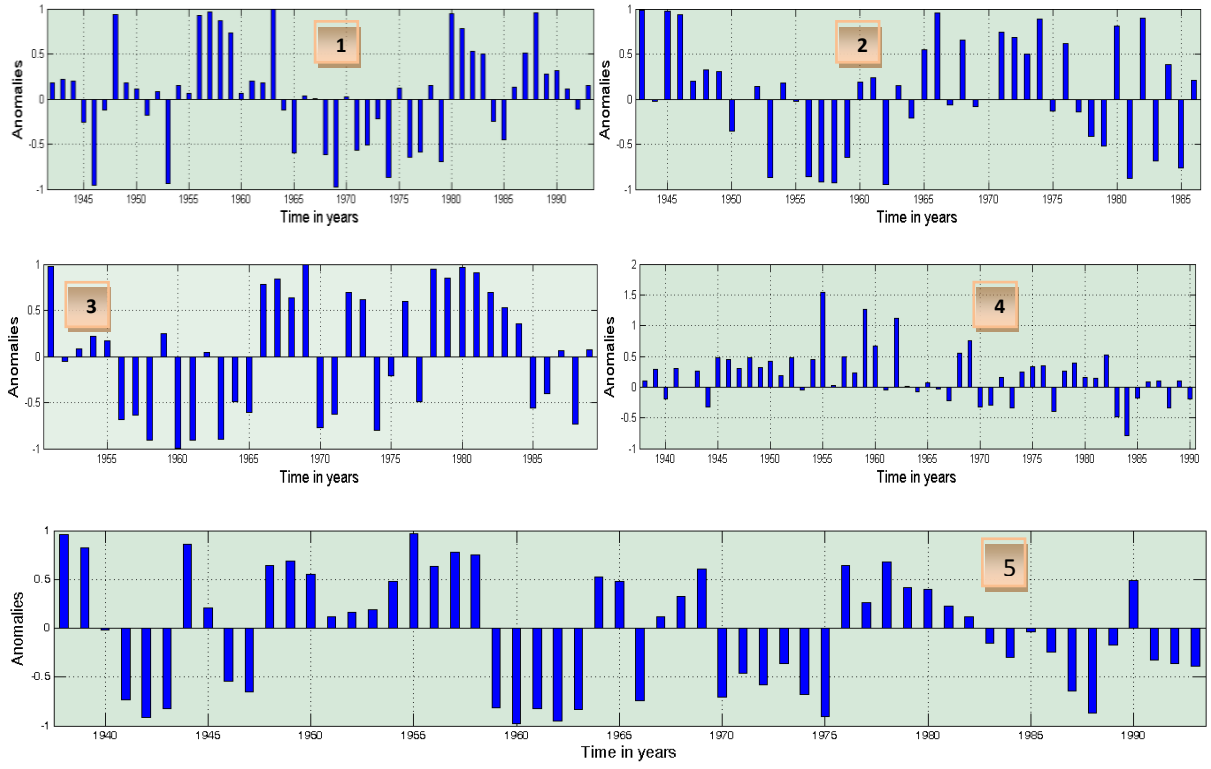

Figure 15B: illustrates the evolution of the standardized rainfall anomaly over Panzangue(1), Goundi(2), Kairoual(3), Radom(4) and for the entire sub-region two (5). Rainfall fluctuates above and below the mean between 1938-1993.The anomalies for the entire sub-region two show rainfall to have been largely below the mean since early 1960s. Variability is mainly due to influence from the ITCZ at its maximum position at 10^{o}N during North African boreal summer.

Figure 15B1, B2, B3, B4 and B5 show the evolution of the standardized rainfall anomaly over Panzangue, Goundi, Kairoual, Radom and the entire region respectively in sub-region two. Rainfall fluctuates above and below the mean during the study period. Thus, there is greater inter-annual variability within this region. This sub-region coincides with the Soudan climate regime typical of Mayo-Kebbi, Tandjilé, Logone Occidental, Logone Oriental, Moyen-Chari, and southern Salamat

with rainy season occurring between May-October. It is also the zone of the main inflow system into the Lake Chad.

Even though sub-region two is located on the lee of the Adamawa and Mandara mountain chains, and forms the hub of inflow Rivers (Chari and Logone) to the lake, inter-annual variability of rainfall as shown in Figure15B above is not as marked as in sub-region three. According to Nicholson (1980), the annual march of the rainy season and rainfall south of the Sahara depends solely on the annual migration of the ITCZ with the zone (zone C in Figure 15C) of maximum precipitation lying approximately at 10^{o} N of latitude south of the surface position of the ITCZ. Sub-region two is centred over this region.

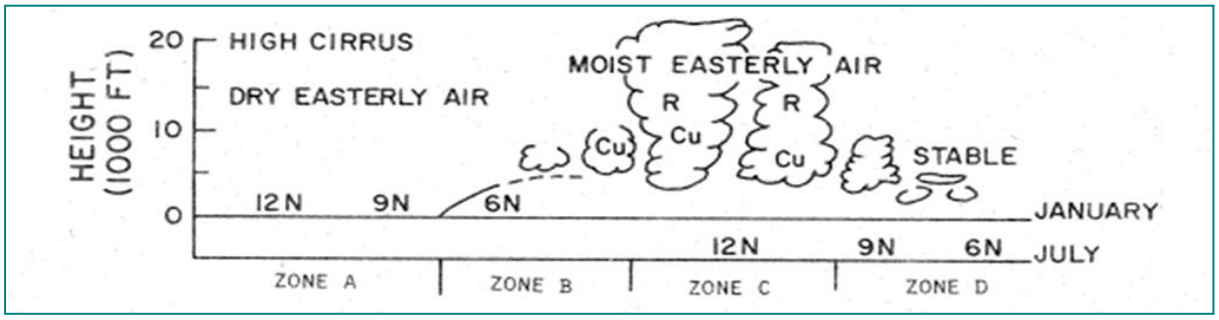

Figure 15C: Inter-tropical convergence zone (ITCZ) model (Griffiths, 1972), including its position in January and July. It is the zone of convergence of the south-westerly low-level winds and Tropical Easterly jet.

Far south of the ITCZ's position (zone D, Figure 15C), rainfall caused by convergence of the south-westerly low-level winds and Tropical Easterly jet convergence decreases sharply. This finding ties with that of Fontaine et al (2010), who found significant reinforcements of the south-westerly low-level winds and Tropical Easterly jet and a northward shift of the African Easterly jet. According to Nicholson *et al*. (2007), a major factor in precipitation variability in the Sahel of West Africa is the latitudinal location of the tropical rain belt. When it is displaced northward, the Sahel experiences a wet year and an anomalous southwest displacement results in dry years.

Chang *et al*. (2000) examined the effect of local sea surface temperatures on atmospheric circulation over the tropical Atlantic sector and postulated that the tropical Atlantic is sensitive to meridional, especially cross-equatorial, SST-gradients. By influencing surface pressure gradients, SST gradients modulate the location of the ITCZ thereby influencing precipitation in Africa and South America. Nicholson *et al*. (2007) argue that SST gradients via inertial instability determine the presence of a strong low-level westerly jet north of the equatorial latitude. This displaces the AEJ northwards into the Sahel which overlies West Africa in the boreal summer, has a core in the mid-troposphere, with speeds of the order of 10 ms^{-1}. This feature is associated with the African Easterly Waves that produce precipitation. The effect of its northward displacement is a simultaneous displacement of the rain-belt (ITCZ) into the Sahel (Nicholson, 2007b). Therefore, as noted in sub-region two and EOF 1, precipitation in this region of the Lake Chad basin owes its variability to the hovering position of the ITCZ during the year.

Sub-region three (Figure 15D) defines the northern Sahel - Saharan zone located between 13^{o}N-24^{o}N of the drainage basin. The Lake Chad water body is located in this sub-region. This is the region with major rainfall deficit since the 1960s (Le Barbe and Lebel, 2001).

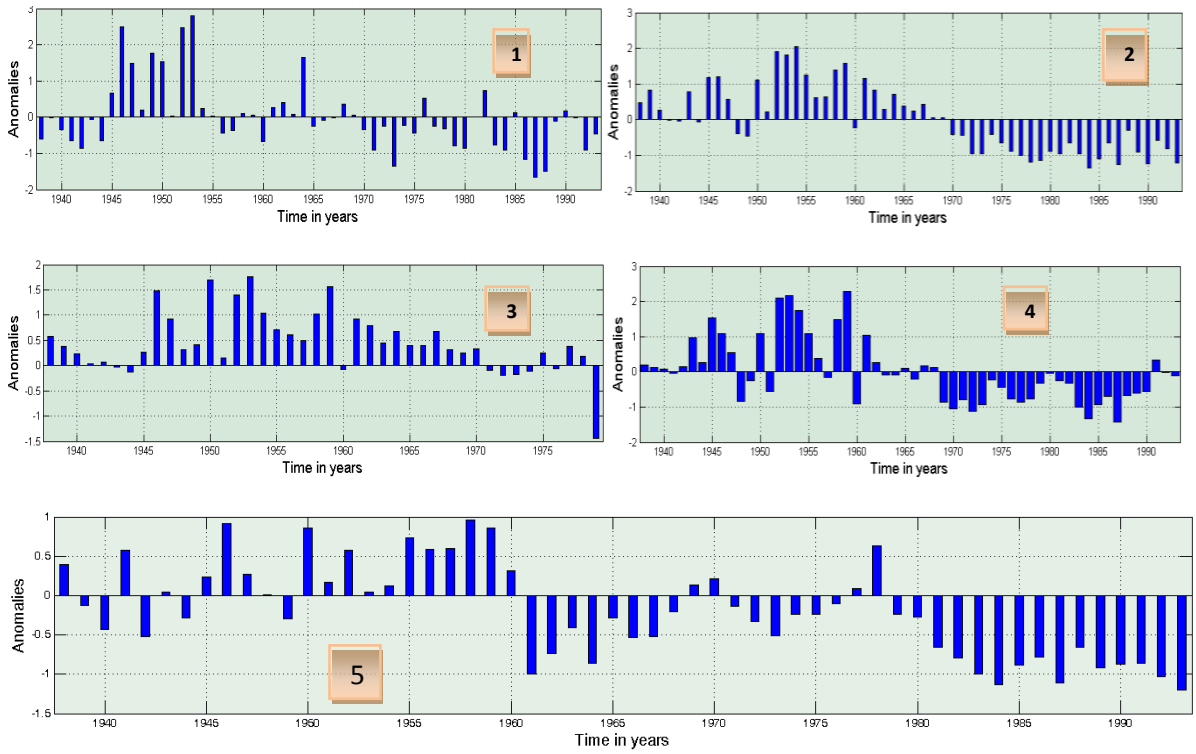

Figure 15D: Show the evolution of the standardized rainfall anomaly in sub-region 3 between 1938 and 1993 for Bilma (1), Faya (2), Ndjamena (3), and Agadez (4) and the entire sub-region three (5). Basically, rainfall remained largely below the mean since the 1960s with greater decline since early 1980s. Variability is mainly a result of differences in moisture gradients driving the AEJ, changes in albedo, and low intensity convection within the ITCZ.

Figure 15D1, D2, D3, and D4 show the evolution of the standardized rainfall anomaly for Bilma, Faya, Ndjamena, and Agadez respectively. Rainfall variability in this region has been widely studied. In terms of atmospheric circulation, Cook (1995, 1997) showed that the African Easterly jet (AEJ) forms over West Africa in summer (July-October) as a result of strong meridional soil moisture gradients. Relatively strong positive geo-potential gradients to the south of the Saharan high pressure belt support extremely strong geostrophic easterly flow, the African easterly jet. Upon approaching 10-15^{o} N, surface easterlies prevail north of the thermal low, forming the dust laden harmattan winds which progress westward within the Saharan air layer. Characteristically, these winds are moisture deficient, and with a greater surface drag, available moisture is absorbed, resulting in increase latent heating. Thus, the associated AEJ, more pronounced moisture divergence below the level of condensation, leading to reduced rainfall and additional surface drying explain rainfall variability in sub-region three.

Janicot (1991) attribute such variability north of 10^{o}N to a more than normal southern location of the ITCZ during the rainy season as well as a reduction in the intensity of convection in the ITCZ. This is logical because the maximum convection occurs at the core of the ITCZ and since only the outer limits of the ITCZ surround this region when it is at its northernmost position, this situation is bound to prevail.

In like manner, Charney (1975) demonstrated that high surface albedo and friction produce strong sinking over the desert by increasing the loss of radiation to space. The atmosphere looses heat and descends adiabatically (warming) in northern Africa. Meteorologically, this sinking motion is associated with high pressure cells and suppresses rainfall.

4.3 Relationship between Tropical Atlantic SSTs and Precipitation Variability

4.3.1 Singular Value Decomposition

The link between precipitation variability in the Lake Chad drainage basin and SST variability over the tropical Atlantic Ocean between 1938 and 1993 was studied using SVD. Results of the analysis showed that precipitation variability in the Lake Chad basin is linked to two spatial patterns of SST. Results are shown on Figures 16, 17, 18 and 19 and in Table 3. In all Figures, correlations significant at 95% confidence level are depicted in black isolines while orange lines show correlations at 99% confidence level. Zero correlations are shown in white isolines. On homogenous and heterogeneous correlation maps, red shading means positive and blue means negative correlations.

Table 3: Shows percentage of explained co-variance and squared covariance fraction; NSC between SST and precipitation co-varying matrix explained by the leading SVD modes and heterogeneous correlations between the co-varying eigenvectors of SST and precipitation.

SVD MODES	SST-Precipitation Covariance (%)	Heterogeneous Correlation	NSC	Squared Covariance Fraction (%)
1	41.3	0.544	0.2	80
2	16.4	0.385	0.07	12.6

The percentage covariance between the SST and precipitation fields and the fractional covariance of the SST-precipitation co-varying matrix explained by the first two leading SVD modes alongside the heterogeneous correlations are presented in Table 3. Two leading modes for SST and three for precipitation are presented on Figures 16 and 17 respectively as homogenous correlation maps. The precipitation (SST) homogenous correlation maps depict the correlation between the filtered precipitation (SST) anomaly at each station (grid point) and the expansion coefficients of the leading eigen-mode of precipitation (SST).

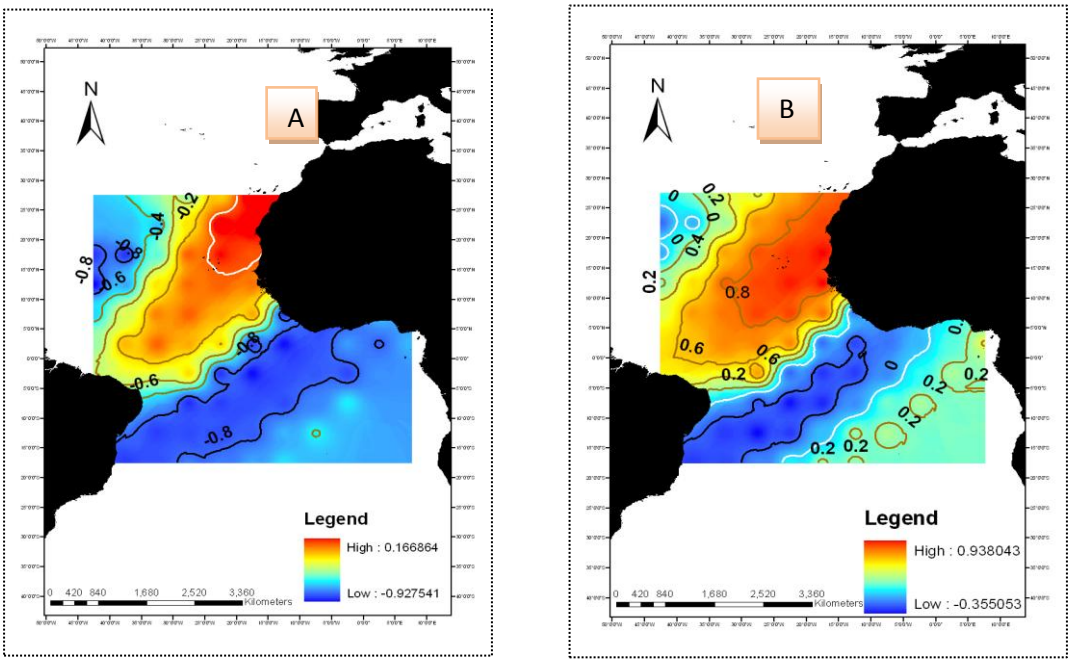

Figure 16A and B: SST homogenous correlation maps. The first eigenvector mode explains 41.3% of the total SST anomaly variance while the second, 16.4%. SST anomalies are higher in the northern tropical Atlantic than in the south with the eastern tropical Atlantic warmer than the west. Red shading means positive and blue means negative correlations. Black isolines represent homogenous correlations significant at 95% confidence level, red = 99% while white = zero correlation.

Figure 16A and B shows homogeneous correlation maps for the first and second SVD modes, respectively, of SST anomalies in the tropical Atlantic Ocean. It is evident that on average, the north-western and southeastern tropical Atlantic experienced opposite inter-annual SST variability if compared to the north-eastern part of the ocean between 1938 and 1993. SST anomaly variability as depicted in the two eigenvector modes is higher in the east of the northern tropical Atlantic than in the west.

Figure 17A, B and C show homogenous correlation maps of stations of precipitation field in the Lake Chad catchment.

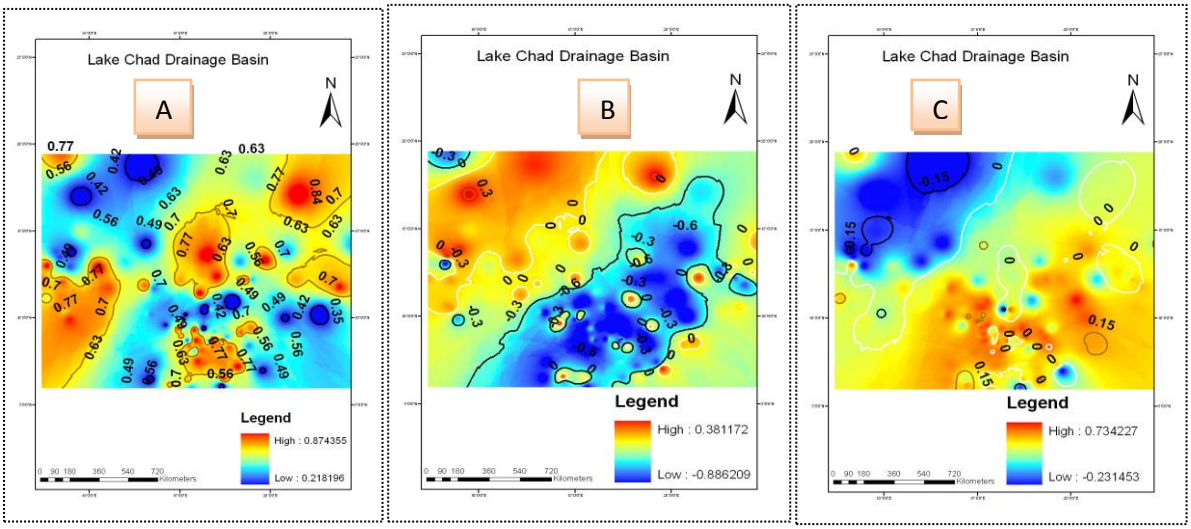

Figure 17A, B and C: Illustrates the first three homogenous correlation maps of SVD modes for precipitation. 17A, B, and C show homogenous maps for SVD modes 1, 2 and 3 respectively. Black isolines represent homogeneous correlations significant at alpha level of 0.05 while the orange lines are significant at 0.01 alpha levels. Zero isolines are represented in white.

These results (homogenous correlation maps) are similar to those found using EOF. For further details, refer to EOF analysis.

The first SVD heterogeneous mode (Figure 18) accounts 41.3% of the covariance between the two fields, squared covariance fraction (SCF) of 80% and NSC of 0.2. SST has positive correlations in the northeastern tropical Atlantic while the corresponding co-varying precipitation mode has positive correlations in the mid-southern portions of the Lake Chad catchment and negatively correlates with the rest of the basin. This region corresponds with sub-region two in CA and EOF 1 of the EOF analysis.

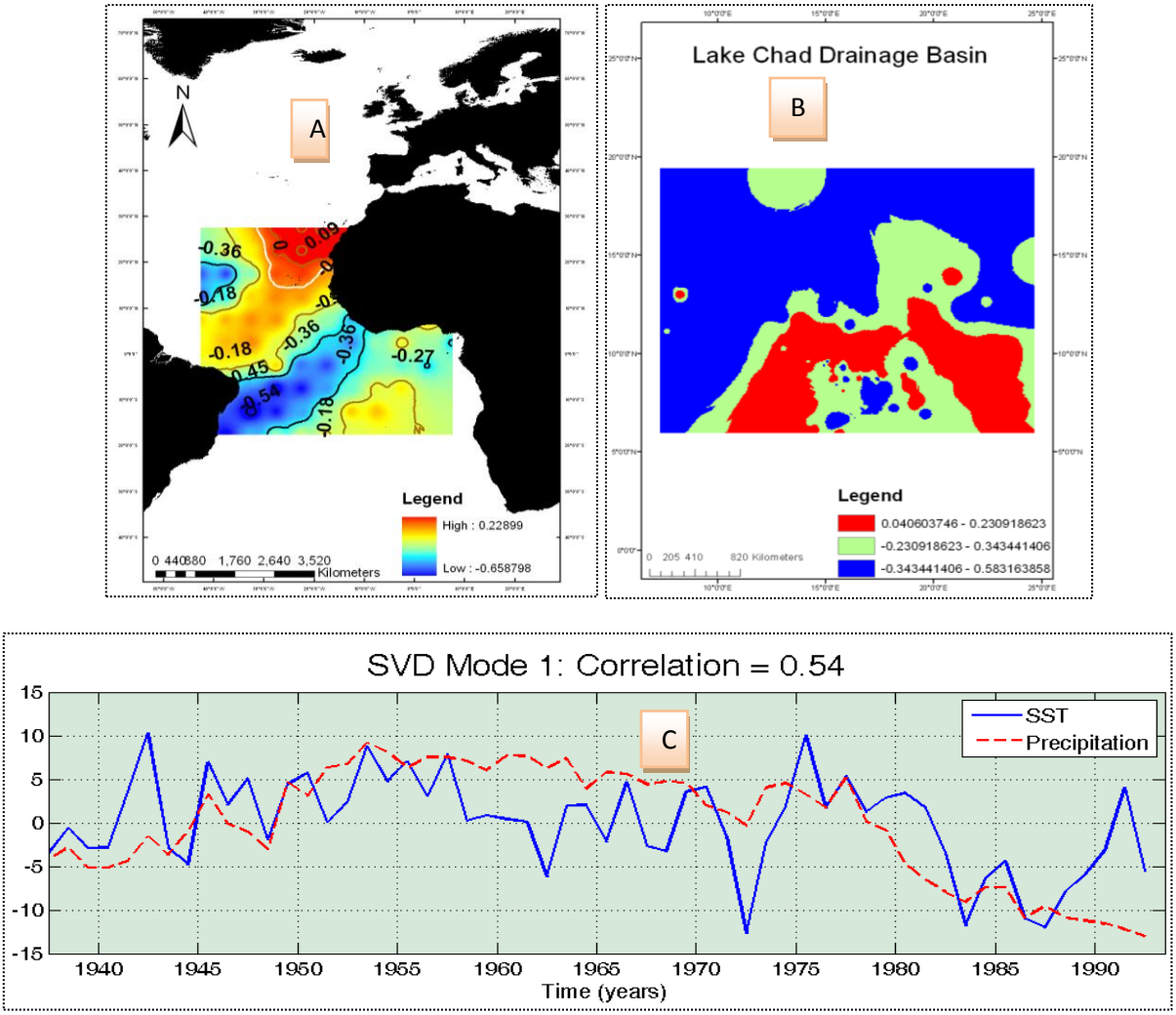

Figure 18A, B and C: Illustrates the heterogeneous correlation maps of SVD mode 1 (positive correlation of 0.54). It has a squared co-variance fraction (SCF) of 80% and NSC of 0.2. SST has positive correlation in the northeastern tropical Atlantic while the corresponding co-varying precipitation mode has positive correlations in the mid-southern portions of the Lake Chad catchment and negatively correlates with the rest of the basin. Black isolines represent correlations significant at 95% confidence level while the orange lines are significant at 99% confidence levels. Zero isolines are represented in white.

The first significant heterogeneous SVD mode between SST and precipitation fields are positively correlated (r = 0.54). This implies that mid-southern parts of the Lake Chad basin tend to have higher precipitation variability when temperatures in the north-eastern tropical Atlantic are abnormally warm. This mode captures long-term precipitation variability in this region of the Lake Chad basin as it can be deduced from Figure 18C. The graph shows long-term trends in precipitation in the basin to be similar to those in the Sahel as shown by Fontaine *et al.* (1998), who noted long-term variability of precipitation in the Sudan-Sahel region to be linked to SST anomalies at near global scales. Precipitation correlates well with SST and has since the 1960s been consistently deviating negatively from normal during the study period. This coincides well with EOF 1 of the EOF analysis (Figure 11).

The heterogeneous correlation map for the second SVD mode (Figure 19) has 16.4% of the explained covariance between the two fields, SCF of 12.6% and NSC of 0.07. SST has positive correlations in the northeastern tropical Atlantic while the corresponding precipitation field has positive correlations in the north-western portions of the Lake Chad catchment (Figure 19B) and negatively correlates with the rest of the basin. Unlike mode 1, SST is more spread out along the eastern portions (western

Africa) of the north tropical Atlantic Ocean (Figure19A). This region in the precipitation field corresponds with sub-region three (Figure 15D) in CA and EOF 2 (Figure 12) of the EOF analysis.

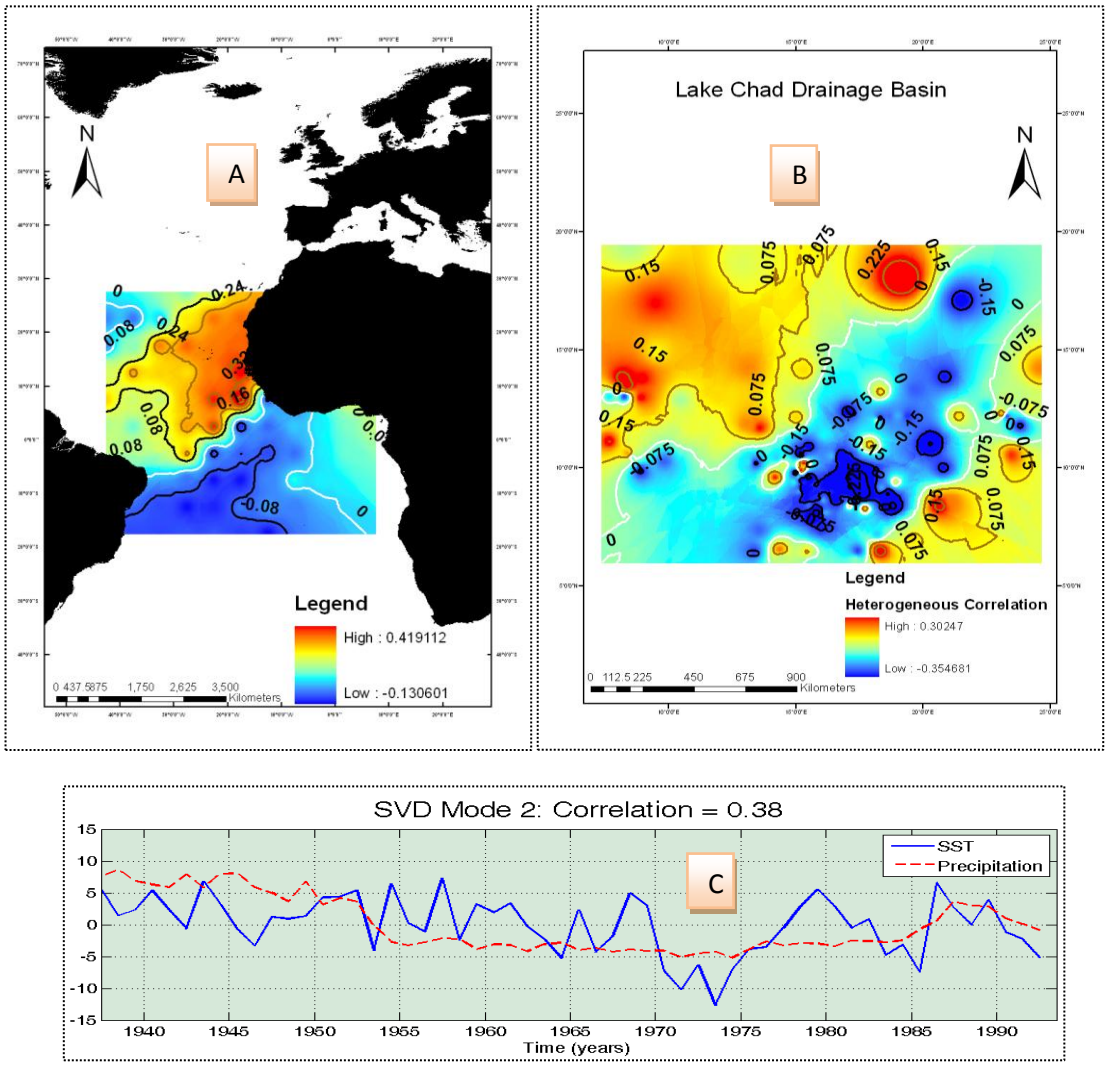

Figure 19A, B and C: Illustrates SVD mode 2 (positive correlation of 0.38). It has 16.4% of the explained co-variance, squared co-variance fraction (SCF) of 12.6% and NSC of 0.07 between the two fields. SST has positive correlations in the northeastern tropical Atlantic while the corresponding co-varying precipitation mode has positive correlations in the northwestern portions of the Lake Chad catchment and negatively correlates with the rest of the basin. Black isolines represent correlations significant at 95% confidence level while the orange lines are significant at 99% confidence levels. Zero isolines are represented in white.

The time series for precipitation and SST related to SVD mode 2 are positively correlated (r=0.38).This implies that the northwestern parts of the basin tend to have higher precipitation variability in years where SSTs in the northern coastline of western Africa especially towards the Gulf of Guinea are abnormally warm. This mode captures inter-annual precipitation variability in this region of the Lake Chad basin as it can be seen from Figure 19C. The graph shows inter-annual trends in precipitation in the basin to be similar to those in the Sahel with a decrease in precipitation since the early 1960s. Precipitation correlates well with SST and has since the 1960s been consistently negative from year to year during the study period. This coincides with eigenvector mode 2 of the EOF analysis.

4.3.2 Canonical Correlation Analysis

The relationship/link between precipitation variability in the Lake Chad drainage basin and oceanic forcing through SST anomalies in the tropical Atlantic is further analyzed by applying canonical correlation analysis (CCA). Prior to application of CCA, the standardized predictor (SST) and predictand (precipitation) data were separately condensed using EOF analyses. The first three EOF modes for SST were retained and accounted 78% of total variance in this field while two EOFs were retained for precipitation and accounted 65% of the total variance.

Results of CCA are shown on Figures 20 and 21. Two significant canonical spatial patterns and canonical vectors were retained for explanation. Figure 20 shows the first pair (CCA1) of CCA spatial patterns and the corresponding canonical vectors. This pair of patterns has a positive maximum canonical correlation of 0.46 and explains 42 % of the variance in the SST field (Figure 20A) and 46% in the precipitation field (Figure 20B).

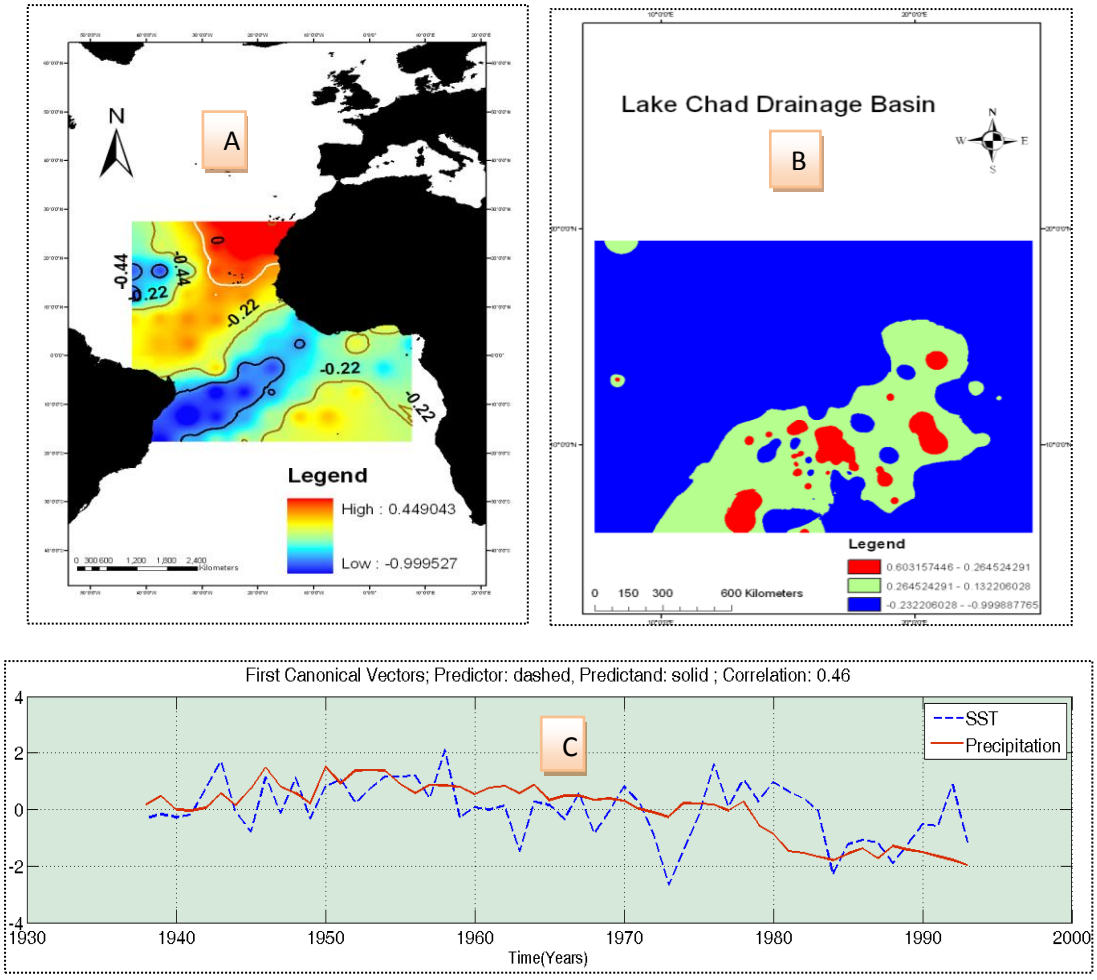

Figure 20A, B and C: First canonical patterns (top) and vectors (bottom). This pair of patterns has a positive maximum canonical correlation of 0.46 and explains 42% of the variance in the SST field (A) and 46% in the precipitation field (B).

Just like the first SVD mode, CCA 1 depicts high SST correlations in the extreme northern tropical Atlantic and decrease from here equatowards. Northeastern tropical Atlantic correlates well with sub-region two of the sub-region analysis. Warm SSTs in the northeastern Atlantic bring high precipitation variability in the mid-southern parts of the Lake Chad drainage basin as there is positive

canonical correlation between the predictor and the predictand. The first canonical vector captures long-term precipitation variability with a consistent declining trend since the early 1960s.

An inter-comparison between CCA1 and SVD1 shows CCA1 to be explicit. This is because prior to application of CCA, the data was reduced for noise by filtering with EOF analysis. By comparing spatial patterns of SVD 1 and CCA 1, it is evident that SVD generalizes the degree of relationship between SST and precipitation in the Lake Chad basin as it engulfs a very large area within the mountain chains in sub-region two of CA. CCA1 clearly defines areas of major linkage between precipitation and oceanic forcing.

Figure 21 shows the second pair (CCA2) of CCA spatial patterns and the corresponding canonical vectors. This pair of patterns has a positive maximum canonical correlation of 0.23 and explains 28% of the variance in the SST field (Figure 21A) and 19.13% in the precipitation field (Figure 21B).

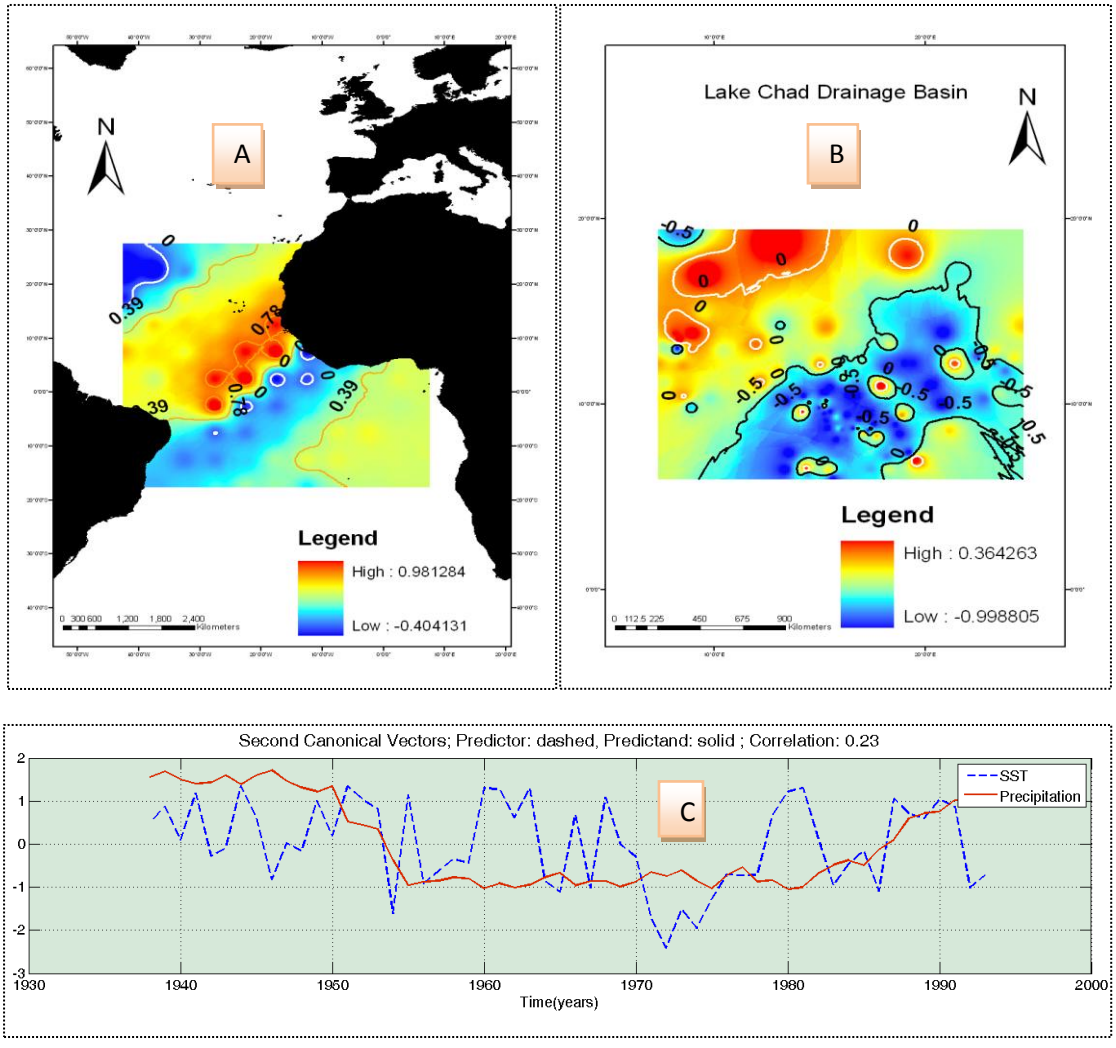

Figure 21A, B and C: Second canonical patterns (top) and vectors (bottom). This pair of patterns has a positive maximum canonical correlation of 0.23 and explains 28.10 % of the variance in the SST field (A) and 19.13% in the precipitation field (B).

SST and precipitation are positively correlated in CCA2. In the SST field, the southeastern coastline of western Africa show positive SST correlations while the corresponding predictand field show positive precipitation correlations in the more northwestern parts in the Lake Chad basin. This implies

that, in years of high SSTs in the southern parts of the northeastern Atlantic, there is a corresponding forcing of high precipitation variability in the northwestern portion of the Lake Chad drainage basin. Just like in SVD1, CCA2 captures inter-annual variability of precipitation in the basin (Figure 21C) with greater negative inter-annual anomalies evident between the late 1950s and late 1980s. CCA2 clearly defines the region of precipitation occurrence due to SST forcing unlike SVD2 where the later defines smaller portions in the southeast of the basin to be influenced by inter-annual SST anomalies. This could result from interpolations or due to amount of variance explained by EOFs prior to application of SVD.

4.4 Spatial-Temporal Relationships between Precipitation and River Discharge

The link between precipitation and discharge variability in the Lake Chad drainage basin between 1948 and 1988 was studied using CCA. The same period for the predictor and predictand variables was chosen to better understand the extent to which discharge relates with precipitation in the Lake Chad basin. Results of the analysis showed that variability in discharge in the Lake Chad basin is linked to two spatial-temporal patterns of precipitation. Results are shown on Figures 22 and 23. Four significant canonical spatial patterns and canonical vectors were retained for explanation.

Figure 22 shows the first pair of CCA spatial patterns and the corresponding canonical vectors. This pair of patterns has a positive maximum canonical correlation of 0.96 and explains 39 % of the variance in the precipitation field (Figure 22A) and 57% in the discharge field (Figure 22B).

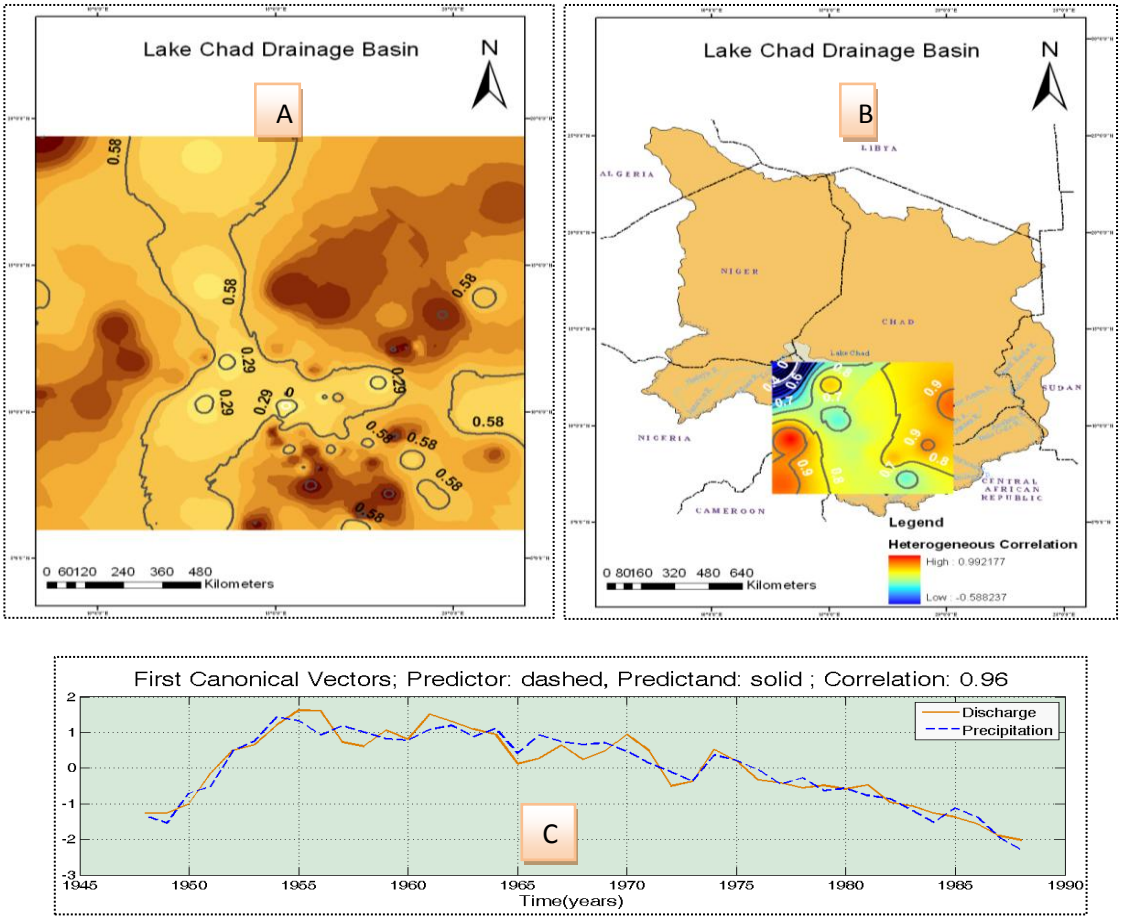

Figure 22A, B and C: First canonical patterns (top) and vectors (bottom). This pair of patterns has a positive maximum canonical correlation of 0.96 and explains 39% of the variance in the precipitation field (A) and 57% in the discharge field

(B). Correlations are significant at 99% and 95% confidence interval and represented by grey and black isolines respectively. Zero correlations are shown in white lines. Red shading means positive and blue means negative correlations

CCA1 depicts positive correlations in the precipitation field. The heterogeneous correlations are greater over the mountain chains of Adamawa and Mandara in Cameroon, Mongo Hills in CAR, and Djebel Mara in Sudan, Air plateau in Niger and Jos plateau in Nigeria (Refer to sub-region one and EOF 3). Discharge exhibits high positive correlations over the southern and southeastern portions of the drainage basin especially over the Adamawa/Mandara and Djebel Mara mountains. Since the two fields are highly correlated positively, variability in precipitation over these mountainous regions impact corresponding long-term fluctuations in discharge for rivers taking rise from these regions such as Wina, Mbere and Pende, originating from Adamawa and Bahr Azoum river from southeastern Chad.

The first canonical vectors capture long-term variability in both fields (Figure 22C). Precipitation has consistently been below the mean since 1970 with a corresponding decline in discharge for rivers over this region from 1948 – 1988.

The second pair of CCA canonical vector (spatial patterns not shown here because through the analysis, it was found that mode 1 and 2 explain well the spatial occurrence of discharge as a result of precipitation) is depicted on Figure 23. With a positive maximum correlation of 0.93, it explains 19% and 16% of the total variance respectively in the precipitation and discharge fields.

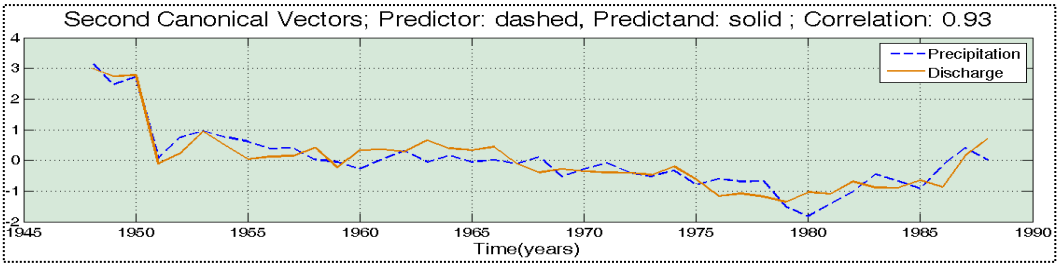

Figure 23: shows the second canonical vector with a positive maximum correlation of 0.93. Discharge response slowly to precipitation variability in the Lake Chad basin. This is evident from the low variability between the two fields as depicted on the graph.

This pair of canonical vectors though with a relatively high positive correlation of 0.93, explains low variability in discharge as a result of variability in precipitation. Figure 23 shows this relationship with low amplitude of variability throughout the period of analysis (1948-1988).

Figure 24 shows the third canonical vector. It has a positive maximum correlation of 0.79, and explains 6.3% and 9.6% of the total variance in the precipitation and discharge domains respectively.

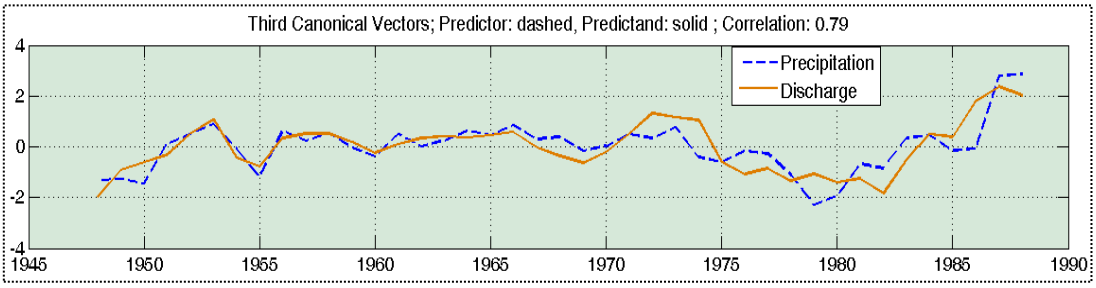

Figure 24: shows the third canonical vector with a positive maximum correlation of 0.79. There is low variability in both fields from 1948-1970 and high variability thereafter. This is indicative that variability in precipitation leads to more variability in discharge.

It can be deduced from Figure 24 that both fields exemplify high variability after 1970. This could be a response from discharge of inter-annual fluctuations in precipitation in the Lake Chad basin from 1970.

The fourth pair of CCA spatial patterns and canonical vectors is depicted on Figure 25. With a positive maximum correlation of 0.68, it explains 4.18% and 5.41% of the total variance in the precipitation and discharge fields respectively.

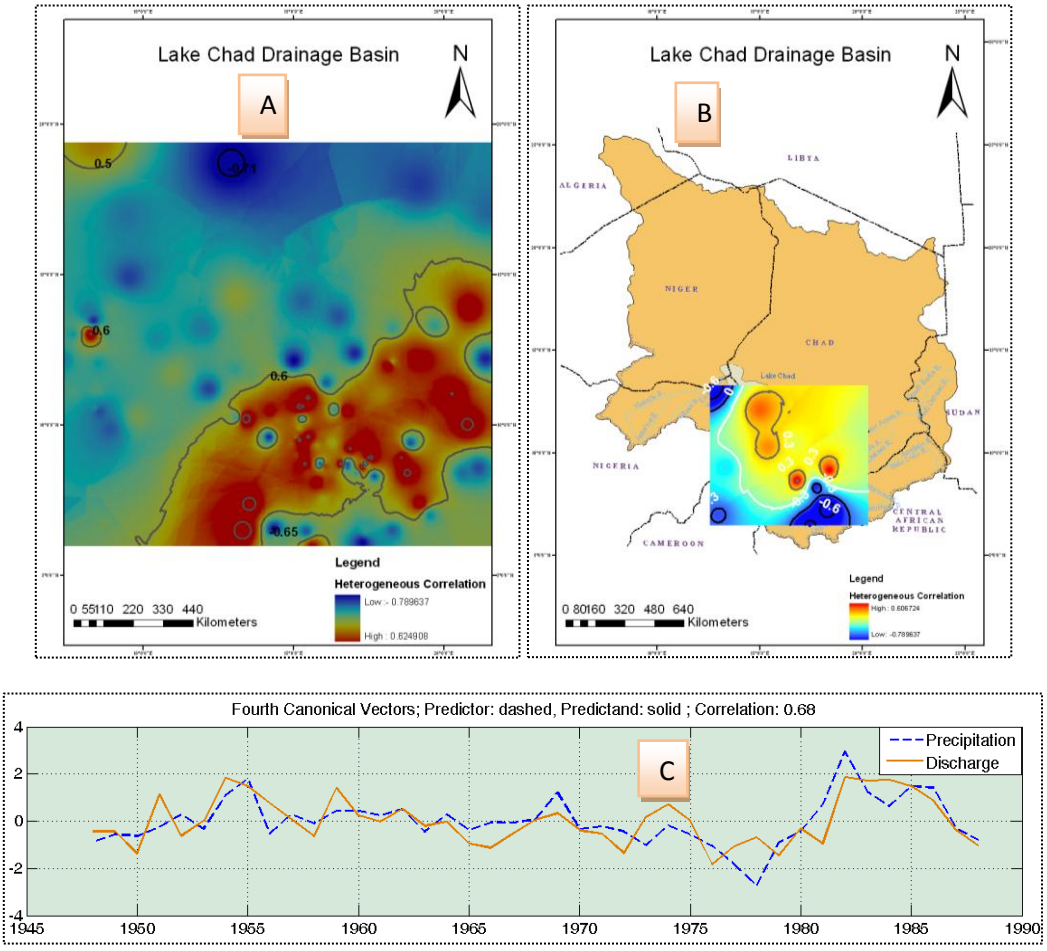

Figure 25A, B and C: Fourth canonical patterns (top) and vectors (bottom). This pair of patterns has a positive maximum canonical correlation of 0.68 and explains 4.18% of the variance in the precipitation field (A) and 5.41% in the discharge field (B). Correlations are significant at 99% and 95% confidence interval and represented by grey and black isolines respectively. Zero correlations are shown in white lines. Red shading means positive and blue means negative correlations

Both fields show positive correlations in sub-region two and EOF 1. The correlations are positive in the mid-southern portions of the basin and negative in the rest of the basin. Variability in precipitation is mainly a result of the inter-annual excursion of the ITCZ which has been found to be due to oceanic forcing through SST anomalies in section 3.3. This results in a corresponding inter-annual variability in discharge for rivers such as the Logone and Chari which contribute more than 60% of inflow into the Lake Chad water body.

The inter-annual variability in precipitation and discharge is captured by the fourth canonical vector (Figure 25C). Both fields fluctuate highly below and above the long-term mean from 1948-1988.

4.5 Analysis of Monotonic Trends

4.5.1 Precipitation

Results of trends analysis are shown on Figures 26 and 27. Stations with no trends are indicated as black circles; those with negative trends are indicated as green dashes, while trends significant at 95% confidence level are represented in red dashes. Out of 113 stations, 42 satisfied the alternative hypothesis of trends presence. All these stations depicted decreasing (negative) trends during the study period and 30 stations displayed negative trends statistically significant at 0.05 alpha level (Appendix A). The Confidence Factor (1 – P-value) indicates the strength of the trends significance. By applying linear regression analysis (to show validity of S), mean precipitation for the entire basin was graphed quantitatively to show temporal characteristics (trends) of rainfall in the basin between 1948 and 1988 (Figure 26).

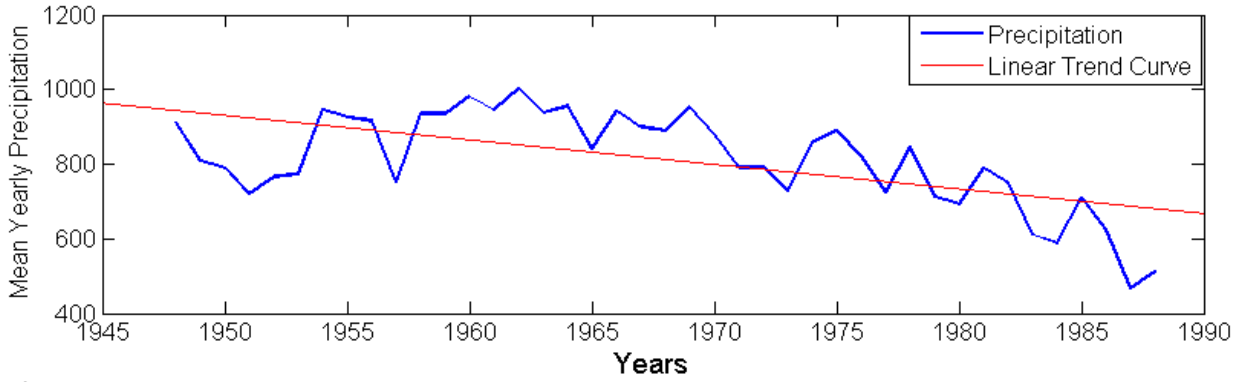

R^2: 0.37 P – value: 5.28e-039 Slope = -6.57

Figure 26: Shows precipitation variability in the whole basin between 1948 -1988. A linear trend curve is fitted to determine direction of the trend. A negative slope of -6.57 is indicative of decreasing trends. R^2 and P – value is indicated at the bottom of the plot. The regression is tested for significance using the one-sample T-test and significance level of 0.05.

By computing a basin average, it is deduced from the plot that there has been a consistent trend towards a decrease in precipitation in the Lake Chad basin as judged from the negative slope of the regression curve. The curve is similar to the long-term precipitation variability graphs identified in SVD/CCA. Precipitation decreased by 19% between 1948 and 1988 with the greatest decrease experienced between 1965 – 1988 accounting for approximately 76% of the basin average.

Coefficients of variation (CVs) for each station were also computed to determine spatial variability of rainfall given that rainfall in the Lake Chad drainage basin experienced a negative trend in all regions. It is evident that stations with greater CVs are located to the north (Appendix A) such as Niger and Chad with 28% and 14% respectively.

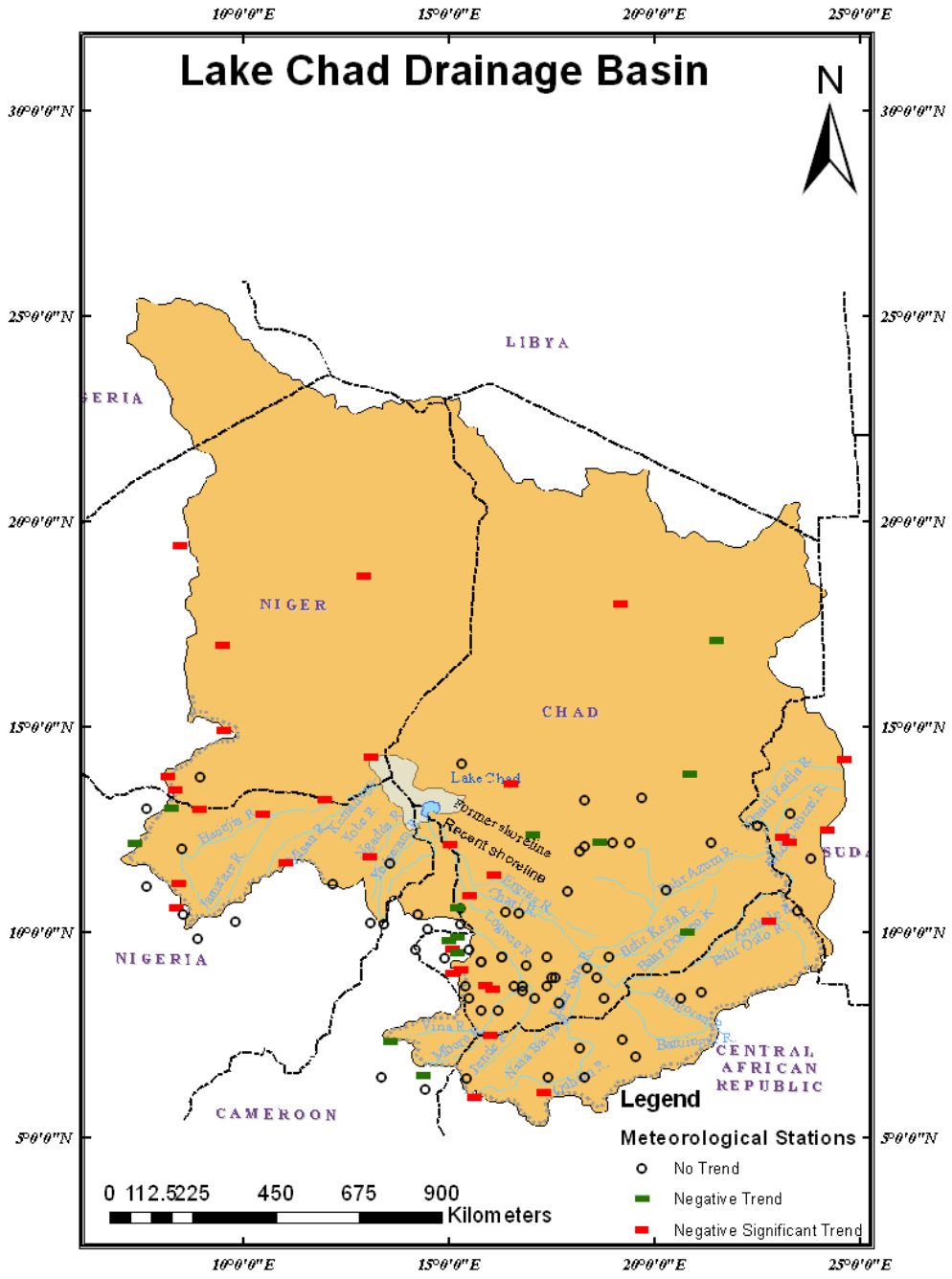

Figure 27: Results of trends analysis with black circles depicting no trends, green dashes for negative trends and red dashes for significant negative trends. Most stations with significant trends are located north/East/West of the drainage basin. 42 stations showed negative trends with 30 stations being significant at alpha level of 0.05.

This finding is in line with that of Le Barbe and Lebel (1997) who noted a decrease in the number of annual rainfall events over the sahelian country of Niger between 1970 and 1989. Least CVs are noticeable in the southernmost regions of the basin in Cameroon and Nigeria where Coe and Foley (2001) noted mean annual rainfall to fluctuate around 1500mm. It is also observed that statistically significant negative trends are concentrated in the northern 2/3 of the basin.

The above tendency for rainfall decline in the drainage basin has its origin. As defined above, the basin is situated in the North African Sahel. Several contributing factors have been put forth to

explain the tendency. Atmospheric circulation patterns, land surface degradation, high evaporation rates as well as its natural location stand as plausible factors.

4.5.2 Discharge

Results of discharge trends analysis are shown on Figures 28 and 29. On Figure 29, Stations with no trends are indicated as red circles; those with negative trends are indicated as green dashes, while trends significant at 95% confidence level are represented in red dashes. Out of 15 stations, 13 satisfied the alternative hypothesis of trends presence. All these stations depicted decreasing (negative) trends during the study period and 11 stations displayed negative trends statistically significant at 0.05 alpha levels (Appendix B). The Confidence Factor (1 – P-value) indicates the strength of the trends significance. By applying linear regression analysis (to show validity of S), mean annual discharge for the entire basin was graphed quantitatively to show temporal characteristics (trends) of discharge in the basin between 1948 and 1988 (Figure 28).

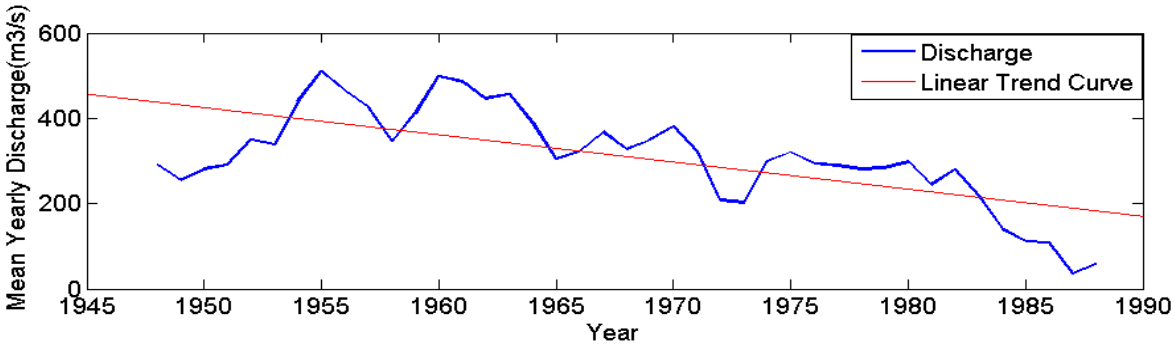

P-Value: 3.6231e-047 $R^2 = 0.4$ slope = - 6.93

Figure 28: Shows discharge variability in the whole basin between 1948 -1988. A linear trend curve is fitted to determine direction of the trend. A negative slope of -6.93 is indicative of decreasing trends. R^2 and P – value is indicated at the bottom of the plot. The regression is tested for significance using the one-sample T-test and significance level of 0.05.

It can be deduced from Figure 28 that discharge decreased markedly between 1948 and 1988. By examining and calculating changes in average discharge over these years, it is evident that discharge decreased by 36% during the study period and 1978 – 1988 alone accounted for approximately 86.7% of total decrease in discharge in the Lake Chad basin.

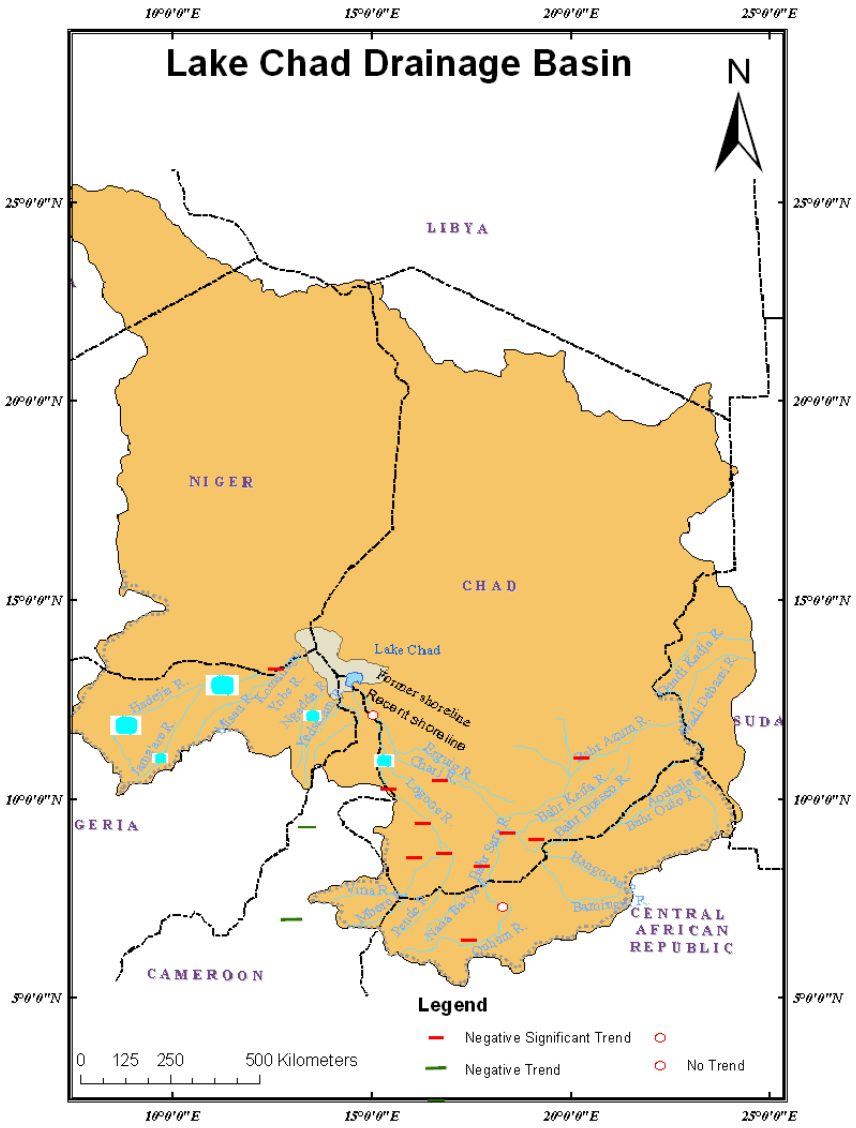

Figure 29: Results of discharge trends analysis with red circles depicting no trends, green dashes for negative trends and red dashes for significant negative trends. The blue-green rectangles represent dams on inflows to the lake. Most stations with significant trends are located over the Chari-Logone river basin. 13 stations showed negative trends with 11 stations being significant at alpha level of 0.05

5 Discussions

Based on results presented in this study, it is clear that rainfall variability in the Lake Chad basin cannot be associated wholly to a single factor. The basin spreads northwards through the soudanian, Sahelian to Saharan climate regimes. Thus, the origin of rainfall is varied and complex as opposed to large-scale synoptic disturbances utilized by researchers to explain rainfall variability in West Africa. Downscaling of meteorological phenomena to a small scale as in the Lake Chad basin re-emphasizes the significance of line squalls and convective clouds in bringing local rainfall in the basin. Dhonneur (1981) postulated that the role played by squall line systems increases to about 80% in the Sahel.

The physiographical configuration of the basin as well as the thermal properties are capable of creating instabilities resulting in strong up and downdrafts in the basin especially on sunny afternoons. Even though this produces minimal rainfall, for purposes of water resources quantification, its role is significant. Continental and oceanic coupling cannot be ignored in explaining rainfall variability over the Lake Chad basin. SVD mode 1 captures long-term precipitation variability in the lee of the Adamawa, Mandara, and Mongo Hills. This zone coincides with the zone of greater convection of the south-westerly monsoon winds and the AEJ within the ITCZ during summer in northern Africa at approximately 10^{o}N. The second SVD mode explains inter-annual precipitation variability in the north-western Sahel –Saharan region at 13^{o}N-24^{o}N. Precipitation variability is mainly a result of feedback mechanisms between land surface changes, differences in soil moisture gradients driving major geostrophic flow, thus, creating subsidence in the Sahel-Saharan air-layer during the year. These changes cause continental convergence north of 10^{o}N latitude which amplifies the influence from oceanic forcing.

Worthy to note is the finding by Fontaine et al (2010). Their results showed rainfall to have increased in north Africa since the mid-1990s with significant northward migration of rainfall amounts($+1.5^{o}$ for the 400mm July to September isohyets whereas deep convection has increased and shifted northwards. The subsidence branch of the northern meridional overturning has also been reinforced and shifted by 1° latitude northward in winter. After 1993-1994, the migration of the Saharan heat low towards northwest has been more marked (+1° to +2° in latitude; −1° to −2° in longitude), whereas its centre intensified at the peak of the tropical rainy season (+10 gpm thickness in the 700–925 hPa layer). These changes are associated with significant reinforcements of the south-westerly low-level winds and Tropical Easterly jet and with a northward shift of the African Easterly jet.
Such a northward shift of the zone of convection implies an increase of rainfall in the Sahel and Saharan latitudes. Rainfall has thus increased in sub-region three unlike conditions before 1993.

A major finding from this study is that precipitation decreased by 19% with the period 1965 – 1988 accounting 75% of the total decrease between 1948 and 1988. However, discharge decreased by 36% within the same period (1948-1988) with the period 1978 – 1988 responsible for 86.7% of total decrease in discharge. This holds that precipitation had been decreasing since 1960s alongside discharge. In section 4.4 of the results, it is evident that precipitation and discharge have very high maximum positive correlations as proved by the CCA pairs. In other dimensions, discharge varies linearly with precipitation between 1948 and 1988. Climate variability contributes in Lake Chad water balance fluctuations but it is not the only cause. Human or other natural phenomena must have interplayed to alter this relationship, with a resulting discrepancy of 17% between decrease in precipitation and discharge.

A major research question then is "what accounted for an extra 17% decrease in stream flow between 1948 – 1988 periods?" Coe and Foley (2001) using an integrated biosphere model and a hydrological model investigated the response of the Lake Chad to climate variability and human water use practices over the last 43 years. According to their findings, irrigation accounted for only 5% of the 30% total decrease in the simulated lake area between 1966 and 1979. However, for the period 1983-1994, the observed water use for irrigation increased four-folds compared to 1953-1979 period. They concluded that human water use accounted 50% of the observed decrease in lake area since the 1960s and 1970s but climate variability still controls inter-annual variability of inflows to the lake.
The extra 17% discrepancy could thus be due to water use demands through irrigation. This can be supported by Figure 29 and Table 4 showing an inventory of irrigation dams over inflow waters to the Lake.

Table 4: shows major irrigation dams over the main rivers contributing inflows to the Lake Chad water body. Note especially their capacities and river basin.

Dam	Capacity(m^3)	Comments	River basin
Zafin Zaki	2 700 million	Suspended	Komadugu-Yobe
Tiga	1 400 million	Control 80% of the flow of the Hadeija river	Komadugu-Yobe
Challawa(1992)	972 million	Control 80% of the flow of the Hadeija river	
Alau Dam	162 million	Supplies city of Maiduguri with 72 million of water	Komadugu-Yobe
Maga dam	680	70% reduction of water supply to the floodplain from the Mandara Mountains	Chari-Logone

Most of these dams were constructed in the late 1980s and early 1990s. These reservoirs are capable of alternating the natural inflow to the lake and thus alternating the lake's response to catchment hydrology and the varying lake area over time. However, an increase in water use could be a response to a drier climate. In order to implement irrigation efficiency controls, one must understand the types of irrigation structures and systems currently used in the basin, as well as the location of dams on inflow rivers (before or after discharge gauge stations), and manner of operation.

Due to absence of data as to rates of evaporation from Lake surface, and transpiration in the basin, its role cannot be assessed but must be born in mind owed to the fact that the basin is located at the edge of the Sahara desert. Groundwater recharge/seepage beneath the lake is a factor to consider. The lake is situated in a water stress environment, implying that the lake could be losing water to underground aquifers especially in the drier periods. Changes in land surface characteristics must be taken into account. Bear land surfaces increase sheet wash instead of infiltration to moisturize the soil. Open surfaces are good for evapo-transpiration. Lake Chad basin is a victim of landscape degradation (GIWA, 2003).

Population growth over the years could have contributed to pressure on water resources. Between 1960 to 1990, the population of the Lake Chad catchment doubled from 16million to 26million (UNEP, 1998).In 1991, the basin contained about 22 million people with an average density of 22 persons/km^2. Today, the population have grown rapidly and being estimated at 37 million people and an average annual growth rate of 2.4% to 2.6% (UNEP, 2004). If population and irrigation demands increase, then water stress in the lake basin will worsen

All these problems (precipitation decrease, discharge decrease, shrinkage of the areal extent of the lake, and damming of rivers) have hindered fair utilization of water resources in the Lake Chad drainage basin. There is a need for integrated water resources management (IWRM) through adaptation and mitigation measures to the above problems. Such measures would entail a change in paradigm that climate variability alone is not responsible for degrading Lake Chad water resources but anthropogenic pressure tends to over amplify forces of climate variability. There must be the laying down of IWRM frameworks for stakeholder participation in these adaptation and mitigation measures towards efficiency in water allocation to riverine countries, distribution and usage amongst different sectors of the society. This can be achieved by enforcing implementation of water roles and regulations outlined in the constitution of the Lake Chad Basin Commission.

6 Conclusions and Recommendations

Multivariate statistical techniques are utilized in this study to divide Lake Chad basin into regions of similar rainfall variability; identify the major spatial-temporal modes of rainfall variability; to examine the link between precipitation variability due to oceanic forcing; demonstrate the occurrence of intricate relationships between precipitation variability and discharge; and make full analyses of monotonic precipitation and discharge trends in the basin between 1948 and 1988.

Using cluster analysis, the basin is descritized into three sub-regions of similar precipitation variability. Sub-region one depicts rainfall variability in the southernmost parts of the drainage basin and spread from west to east. This is the zone of origin (geo-hydrological heads) of all tributaries to rivers feeding the Lake Chad. These stations are concentrated over the mountain chains of *Adamawa* and *Mandara* in Cameroon, *Jos* plateau in Nigeria, *Air* plateau in Niger, *Mongo* hills of CAR, *Djebel Mara* of Sudan and the *Tibesti* highlands of northern Chad. Variability in rainfall is due mainly to the effect of topography on on-caming moisture bearing southwesterly monsoon winds. Sub-region two is mainly concentrated on the lee of the Mandara and Adamawa mountain chains, the southwestern portions of the Djebel Mara in Sudan and north of Mongo hills in CAR. The ITCZ brings summer rainfall in this sub-region. The third sub-region defines the northern Sahel - Saharan zone located between 13^{o}N-24^{o}N of the drainage basin. The Lake Chad water body is located in this sub-region. This is the region with major rainfall deficit since the 1960s. Rainfall variability is mainly a result of the formation of AEJ over West Africa in summer due to strong meridional soil moisture gradients.

Three EOFs are retained to explain spatial-temporal rainfall variability in the basin, accounting for 71% of the total variability in rainfall. The first EOF explains 45.9% of the total variability of precipitation in the drainage basin. It captures inter-annual rainfall fluctuations and coincides well with sub-region two of CA. The second EOF explains 19.13% of the total rainfall variability in the Lake Chad basin. This mode explains inter-decadal or long-term variability in precipitation and coincides well with sub-region three of CA. The third EOF explains 6.22% of the variance. Rainfall variability is orographic in origin and coincides with sub-region one of CA.

A component of precipitation variability in the basin owes its origin to SST anomalies in the tropical Atlantic Ocean. The first SVD heterogeneous mode accounts 41.3% of the covariance between the two fields, squared covariance fraction (SCF) of 80% and NSC of 0.2. SST has positive correlations in the northeastern tropical Atlantic while the corresponding co-varying precipitation mode has positive correlations in the mid-southern portions of the Lake Chad catchment and negatively correlates with the rest of the basin. This region corresponds with sub-region two in the CA and EOF 1 of the EOF analysis. The second SVD mode has 16.4% of the explained covariance between the two fields, SCF of 12.6% and NSC of 0.07. SST has positive correlations in the northeastern tropical Atlantic while the corresponding precipitation field has positive correlations in the north-western portions of the Lake Chad catchment and negatively correlates with the rest of the basin. This region in the precipitation field corresponds with sub-region three in the CA and EOF 2 of the EOF analysis.

By using precipitation as a predictor to discharge in the basin, a very high correlation is found with a strong linear relationship between the two fields. However, a monotonic trends analysis for discharge and precipitation between 1948 and 1988 showed most stations to have experienced significant negative trends and that precipitation decreased by 19% with the 1965-1988 period accounting 76% of the decrease while discharge decreased by 36% with the 1978-1988 period accounting 86.7% of the

decrease. This implies climate variability though is responsible for Lake Chad water balance; the amplitude of water resources degradation is exacerbated by other causes which could be of anthropogenic origin, accounting 17% of the discrepancy. To strive towards sustainable water resources management in the basin, the following recommendations are put forth:

- ✓ Acquisition of high frequency climate data such as daily rainfall
- ✓ Installation of instruments for recording daily evaporation and evapo-transpiration
- ✓ An assessment of irrigation dams on major inflow rivers, types of irrigation practices, location of dams as well as their operation technologies all geared towards efficiency in water uses
- ✓ Assess possibilities of inter-basin water transfer to the lake Chad
- ✓ Ecological assessment of farming methods in the drainage basin which could induce soil erosion and sheet wash after rainstorms
- ✓ Improve monitoring systems for impact of sedimentation on rivers and water courses
- ✓ Population growth is a problem in the basin. Increase in the number of water users in the era of degrading water resources tend to worsen a worsening situation in the basin. This entails a change in paradigm from individualistic towards a holistic approach in water resources management (IWRM).

To achieve these recommendations, short and long-term strategies are needed which must involve addressing current challenges and future needs by adapting to climate variability and mitigating adverse anthropogenic practices on limited water resources in the Lake Chad drainage basin.

7 References

Beauvilain, A. (1996): Les aleas et les Variations Climatiques au Chad: Leurs Consequence sur Evolution des Milieux Naturels et le Developpement du Monde Rural (premiers resultants du projet CAMPUS), Revue Scientifique du Tchad, Vol. 4, no. 1, Numero Special.

Bretherton, C. S., C. Smith, and J. M. Wallace, (1992): An inter-comparison of methods for finding coupled patterns in climate data, *Journal of Climate*, Vol. **5**: pp. 541–560.

Chang, P., Giannini, A., Saravanan, R. (2003): Oceanic Forcing of Sahel Rainfall on Inter-annual to Inter-decadal Time Scales. *Journal of Science*, Vol. 302, No. 5647, pp. 1027-1030.

Chang, P., Saravanan, R., Ji, L and Hegerl, G.C. (2000): The effect of local sea surface temperatures on atmospheric circulation over the tropical Atlantic sector. *Journal of Climate* **13**: 2195–2216.

Charney J.G., (1975): Dynamics of deserts and drought in the Sahel. *Quarterly Journal of the Royal Meteorological Society*, Vol. 101, pp. 193–202.

Coe , M.T and Foley, A.J.(2001): Human and Natural Impacts on The Water Resources of The Lake Chad Basin, *Journal of Geophysical Research, Atmospheres*, Vol. 106,pp.3349-3356.

Cook, K. H., (1994): Mechanisms by which surface drying perturbs tropical precipitation fields. *Journal of Climate*, Vol. 7, pp. 400–413

Cook, K.H. (1995): Understanding perturbations of the inter-tropical convergence zone over tropical continents*:* Global Precipitation and Climate Change, M. Desbois and F. Desalmund, Eds., NATO ASI Series I: *Global Environmental Change*, Vol. 26.

Cook, K.H. (1997): Large-scale atmospheric dynamics and Sahelian precipitation, *Journal of Climate*, Vol. 10: 1137-1152.

Coulibaly, P., Anctil, F., Rasmussen, P and Bobee, B. (2000): A Recurrent Neural Networks Approach Using Indices of Low-Frequency Climatic Variability to Forecast Regional Annual Runoff, *Hydrological Processes*, and Vol. 14 , Issue 15, pages 2755-2777.

Cunnington, W. M and Rowntree, P. R. (1986): Simulations of the Saharan atmosphere—Dependence on moisture and albedo, *Quarterly Journal of Royal Meteorological Society*, Vol. 112: pp. 971–999.

Dai, A., P.T. Lamb, K.E.Trenberth, M.Hulme, P.D.Jones, and P. Xie. (2004): The recent Sahel drought is real, *Journal of International Climatology*, vol.24, no, 1323-1331.

Dhonneur, G., (1981): *Les* amas nuageux mobiles principale composante de la météorologie du Sahel. *La Météorologie*, Vol. 27, pp. 75-82.

Everitt, B.S., (1980): Cluster Analysis. Second Edition, Heinemann Educational Books. London.

Folland, C.K., Owen, J., Ward, M.N and Colman, A. (1991): Prediction of seasonal precipitation in the Sahel Region using empirical and dynamical methods, *Journal of Forecasting* Vol. **10**: pp.21–56.

Folland, C.K., Palmer, T.N and Parker, D.E. (1986): Sahel precipitation and worldwide sea temperatures 1901–1985. *Nature*, Vol. **320**: pp.602–607.

Fontaine, B and Bigot, S. (1993): West African precipitation deficits and sea-surface temperatures, *International Journal of Climatology Vol.* **13**: pp.271–285.

Fontaine, B and Janicot, S. (1996): Sea surface temperature fields associated with West African anomaly types. *Journal of Climate Vol.* **9**: pp.2935–2940.

Fontaine, B., Roucou, P., Gaetani, M., Marteau, R., (2010): Recent changes in precipitation, ITCZ convection and northern tropical circulation over North Africa (1979–2007), *International Journal of Climatology*.

Fontaine, B., Trzaska, S., and Janicot, S. (1998): Evolution of the relationship between near global and Atlantic SST modes and the rainy season in West Africa: statistical analyses and sensitivity experiments, *Journal of Climate Dynamics*, Vol. **14**: pp.353:368.

Gilbert, R.O. (1987): Statistical methods for environmental pollution monitoring. *Journal of Climate*, Volume 10: pp.1137–1152.

Global International Waters Assessment (2003): Lake Chad Basin GIWA Regional assessment 43.

Graham S. (1988) Precipitation: Process and Analysis, John Wiley & Sons Ltd, Baffins Lane, Chichester, W. Sussex, UK.

Griffiths, J.F., (1972): World Survey of Climatology, Vol.10 (Climates of Africa). Elsevier, 604 pp.

Janicot, S., (1991): Spatiotemporal Variability of West African Rainfall. Part II: Associated Surface and Air mass Characteristics, *American Meteorological Society*, Vol. 5, pp.499-511

Kaplan, A., Cane ,M., Kushnir ,Y., A. Clement., M. Blumenthal, and Rajagopalan ,B. (1998): Analyses of global sea surface temperature 1856-1991, *Journal of Geophysical Research*, **103**,No 18:567-18,589.

Kendall, M.G. (1975): Rank correlation methods, Fourth edition, Charles Griffin, London.

Koeppen, W., (1923): Die Klimate der Erde; Grundriss der Klima kunde. De Gruyter, Leipzig, Germany, 369 pp.

Lamb, P. (1978): Large-scale Tropical Atlantic Surface Circulation Patterns Associated with Sub-Saharan Weather Anomalies. *Tellus*, Vol.**30**: pp. 240-251.

Lamb, P. J. (1983): West African water variations between recent contrasting Sub-Saharan droughts, *Tellus*, Vol.35A, 198–212

Lamb, P.J. (1978a): Large-scale Tropical Atlantic surface circulation patterns associated with Sub-Saharan weather anomalies. *Tellus* **30**:240–251.

Lamb, P.J. (1978b): Case studies of tropical Atlantic surface circulation patterns during recent Sub-Saharan weather anomalies 1967 and1968. *Monthly Weather Review*, Vol. **106**: 482–491.

Lamb, P.J. and Peppler, R. A. (1992): Further case studies of tropical Atlantic surface atmospheric and oceanic patterns associated with sub-Saharan drought, *Journal of Climate*, Vol. 5: 476–488.

Le Barbe, L., Lebel,T and Tapsoba, D., (2001): Rainfall Variability in West Africa During the years 1950-1990, laboratoire d'Etude des Transferts en Hydrologie et environment, IRD, Grenobe, France.

Lebel, T. and Le Barbe, L. (1997*):* Rainfall Monitoring During HAPEX-SAHEL; Two Point and Areal Estimation at the Event and Seasonal Scale, *Journal of Hydrology,* Vol. 188-189: 97-122.

Lough, J.M. (1986): Tropical Atlantic sea surface temperatures and precipitation variations in Sub-Saharan Africa. *Monthly Weather Review* Vol. 114: pp.561–570.

Nicholson, S. E and Webster, P. J (2007): A physical basis for the inter-annual variability of precipitation in the Sahel, *Quarterly Journal of the Royal Meteorological Society*, and Vol.133: 2065–2084.

Nicholson, S. E., B. Some and Kone, B. (2000): An analysis of recent rainfall conditions in West Africa, including the rainy seasons of the 1997 El Niño and the 1998 La Niña years, *Journal of Climatology*, Vol. 13, pp.2628-2640.

Nicholson, S.E (1981): Rainfall and Atmospheric Circulation during Drought Periods and Wetter Years in West Africa. *American Meteorological Society*. Vol. 109: No 10, pp. 2191-2208.

Nicholson, S.E (1988): Land Surface-Atmosphere Interaction; Physical Processes and Surface Changes and Their Impacts, prog. Phys.Geogr. Vol. 12: 36-65.

Nicholson, S.E and Palao, J.M. (1992a): A Re-Evaluation of Rainfall Variability in the Sahel. Part I. Characteristics of Rainfall Fluctuations, *International Journal of Climatology*, Vol. 13, pp.371-389.

Nicholson, S.E. (1979): Revised Rainfall Series for the West African Sub-Tropics, *Monthly Weather Review*, Vol.107: 620-623.

Nicholson, S.E. (1980): The nature of rainfall fluctuations in sub-tropical West Africa, Mon.We.Rev, 108,473-487.-1985:Sub-Saharan rainfall 1981-1984, *Journal of Climate*, Vol.24:1388-1391

Nicholson, S.E. (2007a): On the factors modulating the intensity of the tropical rain-belt over West Africa. *Journal of Climate* (in press).

Nicholson, S.E. (2007b). The intensity, location and structure of the tropical rain-belt over West Africa as a factor in inter-annual variability, *International Journal of Climatology* (in press).

Nicholson, S.E., (1980): The nature of rainfall fluctuations in sub-tropical West Africa, *Monthly Weather Review*. 108,473-487.-1985:Sub-Saharan rainfall 1981-1984. *Journal of Climate.* Appl.Meteor, 24, 1388-1391.Soc., 103, 29–46.

Nicholson, S.E., (1988): Land Surface-Atmosphere Interaction; Physical Processes and Surface Changes and Their Impacts. *Progress in Physical Geography*, vol. 12, 36-65.

Paeth, H and Friederichs, P. (2004): Seasonality and time scales in the relationship between global SST and African precipitation, *Journal of Climate Dynamics*, Vol.**23**: 815–837.

Pilon and Cavadias (2002): Power of the Mann–Kendall and Spearman's rho tests for detecting monotonic trends in hydrological series, *Journal of Hydrology*, Vol. 259, Issues 1-4, pp.254-271.

Preisendorfer , R and Barnett , T.P. (1987): Origins and Levels of Monthly and Seasonal Forecast Skill for United States Surface Air Temperatures Determined by Canonical Correlation Analysis, *American Meteorological Society*, Vol. **115** pp. 1825-1850.

Preisendorfer R.W. (1988) Principal Component Analysis in Meteorology and Oceanography, Elsevier, New York.

Richman M.B. (1986) Rotation of Principal Components, *Journal of Climatology*, Vol.**6**:293–335.

Rogerson, P.A (2006): Statistical Methods for Geography: A Student's Guide, second edition, SAGE publications Ltd, London.

Rowell, D.P., Folland, C.K., Maskell, K and Ward M.N. (1995): Variability of summer precipitation over tropical North Africa (1906–92): observations and modeling. *Q. J. R. Meteorol. Soc.*Vol. 121: 669–704.

Rowell, D.P., Folland, C.K., Maskell, K., Owen, J.A and Ward, M.N. (1992): Modeling the influence of sea-surface temperatures on the variability and predictability of seasonal Sahel precipitation. *Geophys. Res. Lett.*Vol. 19: 905–908.

Semazzi, F.H.M., Burns, B., Lin, N.H and Schemm, J.K. (1996): A GCM study of the tele-connections between the continental climate of Africa and global sea surface temperature anomalies. *Journal of Climate*, Vol. **9**: 2480–2497.

Taha, B.M.J., Girard, C., Cavadias, G.S and Bobee, B. (2001): Regional Flood Frequency Estimation, *Journal of Hydrology*, Vol. 254, pages 157- 173.

Thornthwaite, C.W. (1931): The Climates of North America, according to a new classification. *Geographic Review*, Vol. 21,633-655.

UNEP (2004):Fortnam, M.P. and Oguntola, J.A. (eds). *Lake Chad Basin, GIWA Regional Assessment 23*. University of Kalmar: Kalmar, Sweden.

UNEP, *Global environment outlook 2000*, Nairobi: UNEP, 1998, 398.

Uvo and Graham (1998): Seasonal Runoff Forecast for Northern South America: A Statistical Model, *Water Resources Research*, Vol. 34, NO. 12, Pages 3515-3524.

Uvo, C. B. (2003): Analysis and Regionalization of Northern European Winter Precipitation Based on its Relationship with the North Atlantic Oscillation, *International Journal of Climatology*, Vol.23: 1185–1194.

Uvo, C.B., Carlos, A.R., ZEBIAK, S.E., and KUSHNIR, Y. (1997): The Relationships between Tropical Pacific and Atlantic SST and Northeast Brazil Monthly Precipitation, *Journal of Climate*, Vol. **11**: pp. 551-562.

Vincent, M., Andrew, W. R., M. Ward., and Ousamne, N., (2007): Weather Types and Rainfall over Senegal. Part I: Observational Analysis, *Journal of Climate*, Vol.21, 266-287.

Von Storch, H. Burger, G. Schnur, R. & Von Storch, J. S., (1995) Principal oscillation pattern: A review. *Journal of Climate*, Vol. 8, 377–400.

Walker, J., and P. R. Rowntree, (1977): The effect of soil moisture on circulation and rainfall in a tropical model, *Quarterly Journal of the Royal Meteorological Society*, Vol.103, Issue 435, pages 29–46.

Wallace, J. M., C. Smith and C. S. Bretherton. (1992): Singular value decomposition of wintertime sea surface temperature and 500- mb height anomalies. *Journal of Climate,* Vol. **5**: 561–576.

Wallace, J.M; Zhang, Y; Lau, K.H (1993): Structure and Seasonality of inter-annual and Inter-Decadal Variability of the Geo-potential Height and Temperature Fields in the Northern Hemisphere, Journal of Climate, Volume: **6** Issue: 11:2063-2082

Ward, M.N. (1998): Diagnosis and short-lead time prediction of summer precipitation in tropical North America at inter-annual and multi-decadal timescales. *Journal of Climate,* Vol. **11**: 3167–3191.

Westra, S., Sharma, A., Brown, C and Lall, U.(2008): Multivariate Stream flow Forecasting using Independent Component Analysis, *Water Resources Research*, Vol. 44, W02437, doi:10.1029/2007WR006104.

White D. and Richman M. (1991) Climate Regionalization and Rotation of Principal Components, *International Journal of Climatology*, Vol. **11,** 1-25.

Wilks, S.D. (1995): Statistical Methods in the Atmospheric Sciences: International Geophysics Series, Vol. 59. Academic Press, San Diego CA.

Yurdanur, U., Tayfun, K and Mehmet, K (2003): Redefining the Climate Zones of Turkey Using Sub-region Analysis, *International Journal of Climate*, Vol.23: 1045–1055.

Zorita, E., Kharin, V., Von Storch, H. (1992): The Atmospheric Circulation and Sea Surface Temperature in the North Atlantic Area in winter: Their Interaction and Relevance for Iberian Precipitation, *Journal of Climate,* Vol.**5**: 1097-1107.

Appendixes

Appendix A: Summary results of trend analysis for precipitation. P_value associated with S shows the significance of the trend. Rows in green are stations that are not significant

WMO Station	Longitude	Latitude	Elevation (m)	Trend	S	Z	P associated with Z	CV	P associated with S
BILMA	12.92	18.68	355	decreasing	-523	-1.81930131	0.9629	27.631	0.00312
AGADEZ	7.98	16.97	501	decreasing	-316	-1.09785424	0.854272	14.508	0.0024
TANOUT	5.5	19.4		decreasing	-747	-2.59999766	0.85193	26.7063	0.0345
BIRNI-N'KONNI	5.25	13.8	272	decreasing	-1334	-4.64584033	0.75907	9.4072	0.013
MARADI	7.08	13.47	372	decreasing	-1069	-3.72224867	0.7024	9.39032	0.00289
MAGARIA	8.93	12.98	402	decreasing	-1504	-5.2383331	0.62247	11.6578	0.0465
MAINE-SOROA	11.98	13.23	338	decreasing	-1357	-4.72600112	0.5158	11.5602	0.0324
KUTUM	24.6	14.2	1160	decreasing	-615	-2.13994446	0.61003	12.2148	0.025
GARSILA	23.1	12.3		decreasing	-878	-3.05656562	0.96213	10.4007	0.0621
HABILA	22.5	12.6		decreasing	-1033	-3.59677961	0.62456	18.4881	0.046
ZALINGEI	23.3	12.9	900	decreasing	-603	-2.09812144	0.82391	8.8957	0.048
KAS	24.2	12.5		decreasing	-1041	-3.62466162	0.6011	17.2478	0.0845
KUBBUM	23.8	11.8		decreasing	-994	-3.4608548	0.5418	14.8838	0.0124
BOSSEMBELE	17.63	5.27	673	decreasing	-1521	-5.29758237	0.5967	11.8332	0.037
BATANGAFO	18.2	7.2		decreasing	-629	-2.18873798	0.69	13.889	0.0489
NDJAMENA	15.03	12.13	295	decreasing	-117	-0.40428918	0.51298	10.3514	0.0375
MOUSSORO	16.5	13.6	301	decreasing	-762	-2.65227644	0.54734	21.5595	0.014
GUELENGDENG	15.5	10.9		decreasing	-1282	-4.46460725	0.8272	18.5631	0.98
BA-ILLI	16.4	10.5	330	decreasing	-1188	-4.1369936	0.5381	9.93627	0.457
MASSENYA	16.1	11.4	328	decreasing	-732	-2.54771889	0.6187	12.2887	0.0371
MOUNDOU	16.07	8.62	428	decreasing	-1063	-3.70133716	0.7783	21.6272	0.0376
LAI S/P	16.3	9.4	358	decreasing	-1200	-4.17881662	0.86	11.275	0.02827
BEBEDJA	16.6	8.7	395	decreasing	-1192	-4.15093461	0.852	15.0751	0.046
DELI	15.9	8.7	427	decreasing	-1321	-4.60053206	0.5322	14.0889	0.0482
DOBA	16.8	8.7	380	decreasing	-495	-1.72171427	0.53034	10.1114	0.06
BOKORO	17.05	12.38	300	decreasing	-730	-2.54074839	0.61317	12.7716	0.0438
GUIDARI	15.3	9.1		decreasing	-1289	-4.48900401	0.583	19.795	0.0379
BILLIAM OURSY	15.2	10.6	319	decreasing	-1158	-4.03243606	0.482	18.8788	0.0492
TIKEM	15	9.8	325	decreasing	-1184	4.1230526	0.478	14.4646	0.0523
KAIROUAL	15.2	9.5	402	decreasing	-859	-2.99034584	0.931	14.0665	0.053
FIANGA CFPA	15.2	9.9	327	decreasing	-1136	-3.95576052	0.548	17.2172	0.021
SARH	18.38	9.15	365	decreasing	-1028	-3.57935335	0.73	8.68891	0.0454
KOUMRA CT	17.5	8.9		decreasing	-1200	-4.17881662	0.673	13.6259	0.046312
BEKAMBA	17.4	8.7	380	decreasing	-1210	-4.21366914	0.5812	14.204	0.42
HARAZE-MANGUEIGNE	20.8	10	373	decreasing	-1014	-3.53055983	0.5313	10.0214	0.0364
BARO	19	12.2	505	decreasing	-1233	-4.29382992	0.5466	16.2071	0.0478
MAROUA-SALAK	14.25	10.45	423	decreasing	-1416	-4.93163096	0.562	9.74201	0.031
KAELE	14.5	10.1	386	decreasing	-1410	-4.91071945	0.626	8.68954	0.059
MEIGANGA	14.37	6.53	1027	decreasing	-1411	-4.9142047	0.705	7.19645	0.6321
GUSAU	6.7	12.17	463	decreasing	-1266	-4.40884322	0.73	10.4584	0.064
KANO	8.53	12.05	476	decreasing	-1150	-4.004554	0.921	7.08034	0.0864
NGURU	10.47	12.88	343	decreasing	-1010	-3.51661882	0.78	15.8966	0.054

Appendix B: Summary results of trend analysis for discharge. P-value associated with S shows the significance of the trend. Rows in green are stations that are not significant while red means no trend

WMO Station	River	Longitude	Latitude	Elevation (m)	Trend	S	Z	P associated with Z	P associated with S
Lahore	Wina	13	7	1048	Decreasing	-301	-1.822	0.612	0.086
Garoua	Benoue	13.38	9.3	174	Decreasing	-264	-1.59	0.6215	0.0623
Ndjamona	Chari	15.03	12.11	285	No Trend	585	3.547	0.487	
Sarh	Chari	18.41	9.15	355	Decreasing	-419	-2.5389	0.8125	0.0132
Bossangoa	Ouham	17.45	6.47		Decreasing	-488	-2.958	0.597	0.045
Golongoso	Nahr Aouk	19.15	9		Decreasing	-38	-0.2257	0.67	0.0258
Batangafo	Ouham	18.28	7.3		No Trend	562	3.407	0.342	
Bongor	Logone	15.42	10.27	321	Decreasing	-202	-1.2208	0.751	0.0378
Am Timan	Bahr Azoum	20.28	11.03		Decreasing	-113	-0.68	0.214	0.0324
Bousso	Chari	16.72	10.48	325	Decreasing	-129	-2.223	0.94	0.036
Moundou	Logone	16.07	8.53	391	Decreasing	-367	-0.4069	0.57	0.0457
Doba	Pende	16.83	8.65		Decreasing	-68	-1.233	0.8	0.0127
Lai	Logone	16.3	9.4	350	Decreasing	-204	-2.283	0.45	0.046
Moissala	Bahr Sala	17.77	8.33	518	Decreasing	-377	-5.181	0.87	0.038
Bagara Diffa	Komadougou	12.6	13.28	298	Decreasing	-854	-2.653	0.765	0.0374